FINAL REPORT ~ FHWA-OK-22-03

USE OF A NOVEL CONTROLLED RELEASE SURFACE CURING AGENT FOR BRIDGE DECKS PHASE 2

Lichun Chen
M. Tyler Ley, Ph.D., P.E.

School of Civil and Environmental Engineering (CIVE)
Oklahoma State University
Stillwater, Oklahoma

March 2022

OKLAHOMA
Transportation

USE OF A NOVEL CONTROLLED RELEASE SURFACE CURING AGENT FOR BRIDGE DECKS PHASE 2

FINAL REPORT ~ FHWA-OK-22-03
ODOT SPR ITEM NUMBER 2268

Submitted to:
Office of Research and Implementation
Oklahoma Department of Transportation

Submitted by:
Lichun Chen
M. Tyler Ley, Ph.D., P.E.

School of Civil and Environmental Engineering (CIVE)
Oklahoma State University

March 2022

SI* (MODERN METRIC) CONVERSION FACTORS

APPROXIMATE CONVERSIONS TO SI UNITS

SYMBOL	WHEN YOU KNOW	MULTIPLY BY	TO FIND	SYMBOL
		LENGTH		
in	inches	25.4	millimeters	mm
ft	feet	0.305	meters	m
yd	yards	0.914	meters	m
mi	miles	1.61	kilometers	km
		AREA		
in^2	square inches	645.2	square millimeters	mm^2
ft^2	square feet	0.093	square meters	m^2
yd^2	square yard	0.836	square meters	m^2
ac	acres	0.405	hectares	ha
mi^2	square miles	2.59	square kilometers	km^2
		VOLUME		
fl oz	fluid ounces	29.57	milliliters	mL
gal	gallons	3.785	liters	L
ft^3	cubic feet	0.028	cubic meters	m^3
yd^3	cubic yards	0.765	cubic meters	m^3
		NOTE: volumes greater than 1000 L shall be shown in m^3		
		MASS		
oz	ounces	28.35	grams	g
lb	pounds	0.454	kilograms	kg
T	short tons (2000 lb)	0.907	megagrams (or "metric ton")	Mg (or "t")
		TEMPERATURE (exact degrees)		
°F	Fahrenheit	5 (F-32)/9 or (F-32)/1.8	Celsius	°C
		ILLUMINATION		
fc	foot-candles	10.76	lux	lx
fl	foot-Lamberts	3.426	candela/m^2	cd/m^2
		FORCE and PRESSURE or STRESS		
lbf	poundforce	4.45	newtons	N
lbf/in^2	poundforce per square inch	6.89	kilopascals	kPa

APPROXIMATE CONVERSIONS FROM SI UNITS

SYMBOL	WHEN YOU KNOW	MULTIPLY BY	TO FIND	SYMBOL
		LENGTH		
mm	millimeters	0.039	inches	in
m	meters	3.28	feet	ft
m	meters	1.09	yards	yd
km	kilometers	0.621	miles	mi
		AREA		
mm^2	square millimeters	0.0016	square inches	in^2
m^2	square meters	10.764	square feet	ft^2
m^2	square meters	1.195	square yards	yd^2
ha	hectares	2.47	acres	ac
km^2	square kilometers	0.386	square miles	mi^2
		VOLUME		
mL	milliliters	0.034	fluid ounces	fl oz
L	liters	0.264	gallons	gal
m^3	cubic meters	35.314	cubic feet	ft^3
m^3	cubic meters	1.307	cubic yards	yd^3
		MASS		
g	grams	0.035	ounces	oz
kg	kilograms	2.202	pounds	lb
Mg (or "t")	megagrams (or "metric ton")	1.103	short tons (2000 lb)	T
		TEMPERATURE (exact degrees)		
°C	Celsius	1.8C+32	Fahrenheit	°F
		ILLUMINATION		
lx	lux	0.0929	foot-candles	fc
cd/m^2	candela/m^2	0.2919	foot-Lamberts	fl
		FORCE and PRESSURE or STRESS		
N	newtons	0.225	poundforce	lbf
kPa	kilopascals	0.145	poundforce per square inch	lbf/in^2

TECHNICAL REPORT DOCUMENTATION PAGE

1. REPORT NO. FHWA-OK-22-03	2. GOVERNMENT ACCESSION NO.	3. RECIPIENT'S CATALOG NO.		
4. TITLE AND SUBTITLE USE OF A NOVEL CONTROLLED RELEASE SURFACE CURING AGENT FOR BRIDGE DECKS PHASE 2		5. REPORT DATE Mar 2022		
		6. PERFORMING ORGANIZATION CODE		
7. AUTHOR(S) Lichun Chen, M. Tyler Ley		8. PERFORMING ORGANIZATION REPORT Click here to enter text.		
9. PERFORMING ORGANIZATION NAME AND ADDRESS Oklahoma State University Civil and Environmental Engineering 241 Engineering North Stillwater, Oklahoma 74078		10. WORK UNIT NO.		
		11. CONTRACT OR GRANT NO. ODOT SPR Item Number 2258		
12. SPONSORING AGENCY NAME AND ADDRESS Oklahoma Department of Transportation Office of Research and Implementation 200 N.E. 21st Street, Room G18 Oklahoma City, OK 73105		13. TYPE OF REPORT AND PERIOD COVERED Final Report Oct 2018 - Sep 2021		
		14. SPONSORING AGENCY CODE		
15. SUPPLEMENTARY NOTES Click here to enter text.				
16. ABSTRACT This report focuses on establishing methods to compare different curing methods and then determining how the timing of wet curing impacts the quality of the concrete in different evaporation environments. Chapter 2 uses electrical resistivity to non-destructively measure the moisture within concrete as it hydrates and correlates this to other measurements. Chapter 3 extends the electrical resistivity to evaluate how delays in the application of wet curing will impact the performance of bridge decks. The resistivity measurements provide new insights that are not easily obtained with other techniques and provide direct insights into the moisture change. The resistivity measurements over time are shown to correlate with the porosity, degree of saturation (DOS), and a novel tensile strength test. Chapter 4 provides an update on the use of Pulp Cure in the field and how modifications to the equipment can be used to make the application easier and more practical.				
17. KEY WORDS **concrete, curing, pulp cure**		18. DISTRIBUTION STATEMENT No restrictions. This publication is available from the Office of Research and Implementation, Oklahoma DOT.		
19. SECURITY CLASSIF. (OF THIS REPORT) Unclassified		20. SECURITY CLASSIF. (OF THIS PAGE) Unclassified	21. NO. OF PAGES 85	22. PRICE N/A

Form DOT F 1700.7 (08/72)

Table of Contents

List of Figures

viii

List of Tables

CHAPTER 1: OVERVIEW OF THE DOCUMENT

ODOT is interested in improving the quality of the wet curing of their bridge decks. This report

first focuses on establishing methods to compare different curing methods and then determining

how the timing of curing impacts the quality of the concrete. Chapter 2 establishes new methods

to non-destructively measure the moisture within concrete. Chapter 3 uses the technology and

methods established in Chapter 2 to evaluate how delays in the application of wet curing will

impact the performance of bridge decks in different drying environments. Chapter 4 provides an

update on the usage of Pulp Cure in the field and gives insights into new equipment and

modifications in the material to improve the usage and lower the cost of the material. A

discussion about possible changes to ODOT practices is included throughout the document.

CHAPTER 2: Using Electrical Resistivity to Predict early age DOS and tensile strength of mortar

2.1 Introduction

The hydration reaction dissolves materials, consumes water, releases heat, and creates solid material through chemical reactions. This work examines how curing in dry air, sealed conditions, and wet curing changes the degree of saturation or moisture level as well as the tensile strength of the concrete. This is determined by measuring the electrical bulk resistivity from an alternating current of a known frequency. This work investigates changes caused by drying by comparing the resistivity at different distances from the surface. These differences in resistivity correlate to changes in the measured porosity, degree of saturation, and the tensile strength. This shows that resistivity is an elegant, non-destructive, economical, rapid, and quantitative measurement that provides important insights into curing mortar mixtures for controlled systems.

The purpose of curing is to minimize moisture loss and retain enough heat to promote the hydration reaction [1, 2]. Curing impacts the formation of hydration products and the development of the microstructure. The microstructure is essential to the physical properties such as porosity, permeability, strength, shrinkage, and creep [3-5]. As a result, it would be valuable to have a low cost method that could be used to evaluate the effectiveness of curing. Studies have investigated the influence of different curing methods such as wet curing and air curing on the compression strength, durability, and resistance to chloride transport [3,6,7]. A study by Hajibabaee has shown that wet curing increases the resistance to ingress of external chemicals compared with air curing or curing compounds [10]. However, those studies were carried out on concrete samples after 28 d of hydration. While this work is useful, more

information is needed about changes in the first 72 h of hydration. Also, more information is needed to determine how curing impacts the sample over the depth with time. Studies have shown that a moisture gradient forms with a drying surface of the sample and this moisture difference will further generate non uniform hydration and therefore a different microstructure of the material [12]. As a result, the influence of curing at the surface is of great importance to the ultimate properties of the materials.

Many studies have used electrical resistivity to measure the process of cement hydration [13-18]. Previous work monitored the electrical resistivity of cement paste during the first 30 h of hydration and showed that resistivity could be used to follow the stages of hydration of cement paste and also give insights into hydration product formation [15]. A study by Xiao shows that electrical resistivity is sensitive to the pore structure change as measured by mercury intrusion porosimetry (MIP) at 2h and 24h of hydration [17]. Since the measurement of electrical resistivity is flexible, effective, nondestructive, it may be able to be used to make continuous measurements of a sample in a simple and low cost manner [15-18]. As a result, electrical resistivity has the potential to examine curing methods and the corresponding impacts on the concrete microstructure and properties. Besides measuring the resistivity directly, the overall resistivity of a composite material can also be described by the general effective media (GEM) model [19][20] and calculated using the capillarity porosity, percolation threshold, formation factor, magnificent coefficient, for the cementitious material in question [21], however, these measurements are not easy to obtain and at this time these measurements have not been generalized for a wide range of materials.

The goal of this study is to use electrical resistivity to make direct measurements of the influence of different curing methods on hydration and material properties over the first 72 h of hydration.

The change in the porosity, degree of saturation (DOS), and the splitting tensile strength over the first 72 h of hydration are investigated for air, sealed, and wet curing methods at different depth of the sample. The results suggest that the DOS, porosity and tensile strength of the sample can be correlated to the resistivity from 12h to 72h. A linear relationship between DOS and resistivity was established at different times of hydration and was applied to predict the DOS of the sample from resistivity. This means that resistivity measurements could be used to determine the effectiveness of different curing methods and provide insights into the properties of the sample.

2.2 Experimental Investigation

2.2.1 Materials & Mixture Design

The mortar mixture in this study was prepared according to ASTM C305 [22] with a w/cm ratio of 0.45. The mixture proportion by volume is shown in Table 1. The cement used in this study met the requirements of an ASTM C150 Type I Portland cement. The fine aggregate used for the mortar mixture was a locally available natural sand and met the requirements of ASTM C33. The Blaine of the cement is 3560 cm^2/g and the free lime content is 1.4%. The chemical compositions of the cement are shown in Table 2.

Table 2-1. Mixture proportion of mortar

	Cement	Water	Fine Aggregate	Air
Volume (%)	18.5	23.4	56.7	0.4

Table 2-2. Chemical composition of cement

	SiO_2	Al_2O_3	Fe_2O_3	CaO	MgO	SO_3	Na_2O	K_2O	C_3S	C_2S	C_3A	C_4AF	LOI
Cement (%)	21.1	4.8	3.1	64.5	2.33	3.2	0.17	0.58	50	23	7	9	2.6

4

t2.2.2 Electrical resistivity test

As shown in Figure 2-1, the plastic cylinder molds have a diameter of 6 inch and were 9 inch tall. The cylinders used seven layers of 4-40 threaded stainless steel rods (0.1 inch in diameter, and 40 threads per 1 inch). Each layer used two rods with a horizontal spacing of 3.65 inch and a vertical spacing of 0.5 inch. The steel rods were installed through the molds and were stabilized and sealed with glue before the mortar was placed. The configuration of the specimen is shown in Figure 1. Mortar was used to fill the mold to 8 inch in height. The top 1 inch was not filled to allow different curing methods to be applied. The mortar was placed in three layers. For each layer, the sample was consolidated for 10 s with a vibrating table at a frequency of 60 Hz to remove entrapped air and to promote a good bond with the threaded rod.

During hydration, water is consumed and the sample shrinks [23]. This volume change may form a gap between the mold and the edge of the sample. To ensure that the drying is only from the top of the sample and not from the edges, the edge of the fresh mortar was sealed with plastic wrap and covered by mortar. More details can be found in Appendix A.

Figure 2-1 labels:

Mortar surface

1" empty volume

0.5"

6 spaces at 0.5"

3.65"

6"

9"

9"

6"

Perspective View

Cross Section
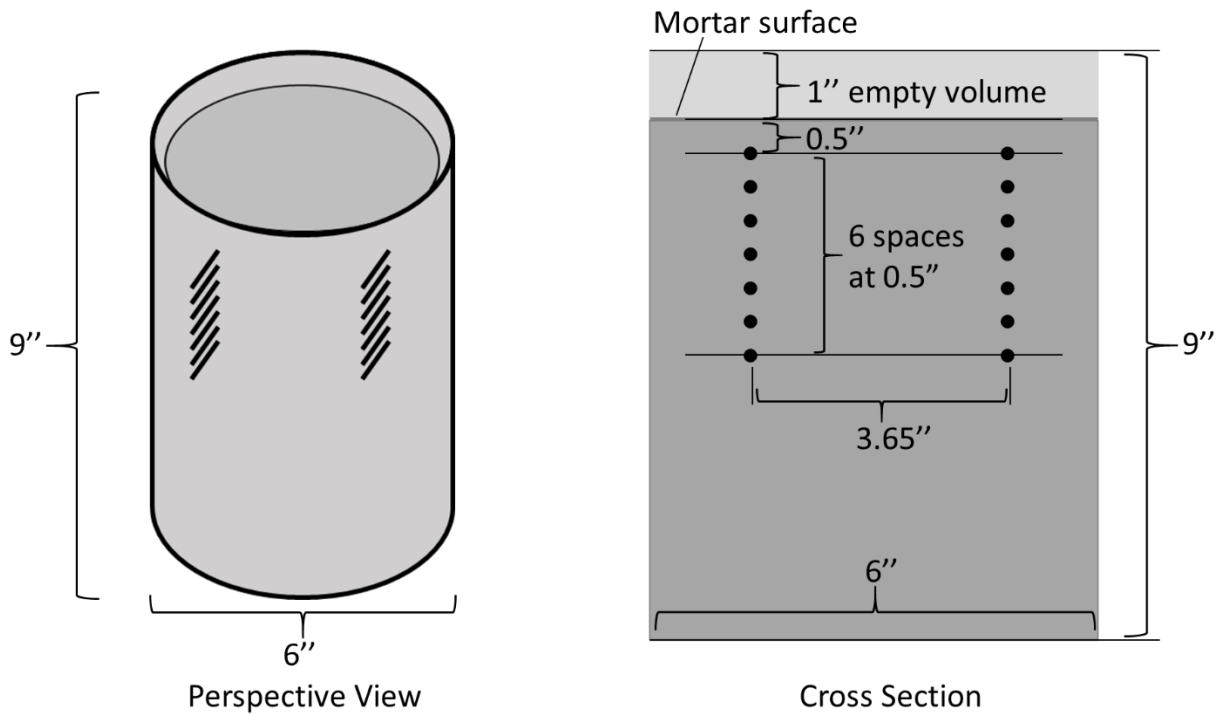
Figure 2-1. Configuration of the mortar sample for resistivity measurement

This study investigated wet curing, sealed curing, and air curing. All three curing methods were conducted in an environmental chamber with a temperature of 73°F and humidity of 50%.

After the samples were cast into molds, curing methods were applied on the surface of the sample. In the wet curing, three layers of water-soaked burlap were placed on the surface and then the surface of the mold was sealed with aluminum tape. Every day the burlap was removed and soaked with water and replaced on top of the sample. In the sealed curing, the mold was covered with aluminum foil and sealed with aluminum tape to prevent moisture loss. The air curing method leaves the sample open to the 50% RH environment.

The resistivity was measured between the rods every 10 minutes through the hydration process. The circuit for the resistivity measurement was programmed with the Arduino platform. An Arduino Mega 2560 was used as the central processor with a 12-Bit impedance converter AD5933. In this research, a

6

frequency of 30 kHz was used. This was chosen because at this frequency the imaginary part of the impedance is close to zero. The system was calibrated with a 100-ohm resistor. The calibration process was to calculate the Gain Factor of the system based on a known resistor. The Gain Factor can then be used to calculate the resistivity in future measurements. The detailed calculations for these measurements are included in Appendix B.2. Five multiplexers were used to measure 80 channels simultaneously. The results were recorded on an SD card and retrieved for analysis. More details about the additional hardware and the raw data process of impedance can be found in Appendix B.1.

Since the frequency range selected has forced the imaginary impedance to close to 0, the measured impedance is also called the bulk resistance of the mortar sample. The unit of the measured bulk resistance is ohm. To get the resistivity of the mortar sample, Equation 1 was used.

$$Resistivity = bulk\ resistance\ (\Omega)*A\ (inch^2)\ /\ L\ (inch)\ \Omega*inch \qquad Equation\ 1.$$

In Equation 1, A is assumed to be the rectangular cross-sectional area of the electrode perpendicular to the signal. The area is taken as 12 $inch^2$, since the electrode is 0.1 inch in diameter and approximately 4.7 inch long. The distance between the electrodes, L, is 3.6 inch.

2.2.3 Mass change

The mass of the wet, sealed, and air curing samples over the first 72 h of hydration was measured and recorded every hour. The percentage of mass change was then obtained with Equation 2.

$$\%\ Mass\ Change = \frac{M_n - M_i}{M_i} \times 100 \qquad Equation\ 2.$$

2.2.4 Porosity and degree of saturation (DOS) test

The porosity and degree of saturation (DOS) [24] are investigated to support the resistivity measurements. The porosity illustrates the microstructure development and the DOS shows the amount of moisture within the sample. The DOS is a critical factor in promoting early hydration within the sample [25-29]. Other research shows that hydration ceases at a relative humidity of about 80% due to negative capillary pressure that opposes the reaction [30].

The mortar samples for the porosity and DOS measurement were cast into tubes with 1inch diameter by 4.5 inch tall. Each tube was filled with three layers of mortar. The mortar was from the same mixture as the one for the resistivity measurement. The wet cured DOS samples were stored in a fog room with a constant humidity of 100% and temperature of 73°F with its surface open to the environment. This is because the surface area of the container is too small to apply wet burlap. The sealed curing and air curing were conducted in an environment with 50% humidity and 73°F temperature. In the sealed curing, the sample top was sealed with the lid for the tube.

The porosity and DOS were measured when the samples had hydrated for 12 h, 24 h, 48 h, 72 h, and 96 h. When the sample reached the designated hydration time, it was demolded and cut into 3 segments that were each 1.5 inch tall. This means that the distance to the midpoint of each segment was 0.75 inch, 2.25 inch, and 3.75 inch from the sample surface. This was done so that the porosity and DOS of each segment could be compared to the resistivity measurements at similar depths.

2.2.4.1 Determining the porosity and degree of saturation (DOS)

The porosity and DOS were determined by ASTM C642 with some minor changes where the samples were saturated within a vacuum chamber at pressure of 37mmHg±5mmHg instead of boiling in water. Equation (3) and (4) were used to calculate the porosity and degree of saturation (DOS), where W_i is the initial weight of the sample, W_d is the oven dried weight at 230 °F, W_{sa} is the saturated surface dried

8

(SSD) weight, W_{su} is the weight of the sample while the sample is suspended in water, it's equal to the difference between the sample weight and its buoyant force.

$$Porosity = \frac{W_{sa} - W_d}{W_{sa} - W_{su}} \times 100 \qquad \text{Equation 3.}$$

$$DOS = \frac{W_i - W_d}{W_{sa} - W_d} \times 100 \qquad \text{Equation 4.}$$

2.2.5 Splitting tensile strength

The splitting tensile strength test is performed according to the previous work by Robertson, B., and Dickey, M. [31][32]. The detailed calculation of the strength and assumptions can be found in the Appendix D. The mortar samples for splitting tensile strength were cast into 6 inch diameter by 3 inch tall plastic cylinders. Metal plates were fixed into the mold to form 2 notches with a 30° angle at the sample surface along its length shown in Figure 2-2 (a). The mold was filled in 2 layers and vibrated for 10 s on the vibration table at 60 Hz. The samples were cured the same way as the resistivity samples.

After the mortar sample hydrated for 72 h, the sample was demolded and split with a hydraulic press as shown in Figure 2-2 (b). The loading platen has the same dimensions as the notches. The splitting test was conducted in this way because the sample failure is caused by the tension forces caused by the loading platen being pushed in compression and pushing on the angled inserts. The platen was loaded at a rate of 50 lbf/min. Each curing method used 5 samples for this test. The samples that did not split at the notches were excluded from the strength calculation. Calculation details are included in Appendix D.

9
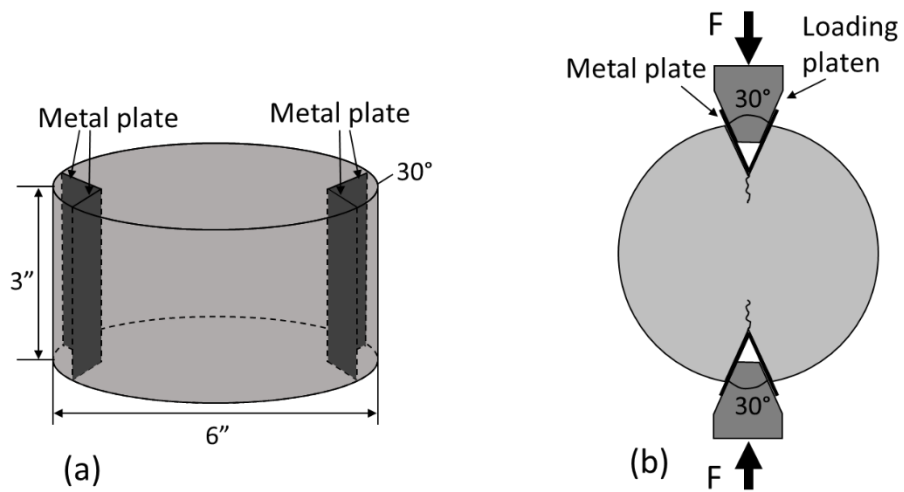
Figure 2-2. Schematic diagrams of (a) mold for splitting tensile strength test and (b) mortar sample under splitting test.

2.3 Results and Discussion

2.3.1 Resistivity response over time

The average resistivity along the sample depth of the three curing methods is shown in Figure 3. Every curing method shows growth in resistivity over time and the resistivity curve of different curing methods presents a similar shape. The similar shape of resistivity growth is likely caused by hydration reactions and consumption of water over time. This will be discussed more in the document over these mechanisms. As the hydration reaction proceeds, free water is consumed to form hydration products as the mixture changes from a slurry to a solid. As a result, the average resistivity of the mortar specimen increases with hydration. The air curing shows the highest resistivity followed by the sealed sample, and then the wet cured sample has the lowest resistivity. The difference in resistivity could depends on several factors including the amount of moisture in the pores, ion concentration in the pores and the tortuosity of the pore network. In this work, the moisture amount and the porosity of the samples are examined. This will be discussed further in the paper.
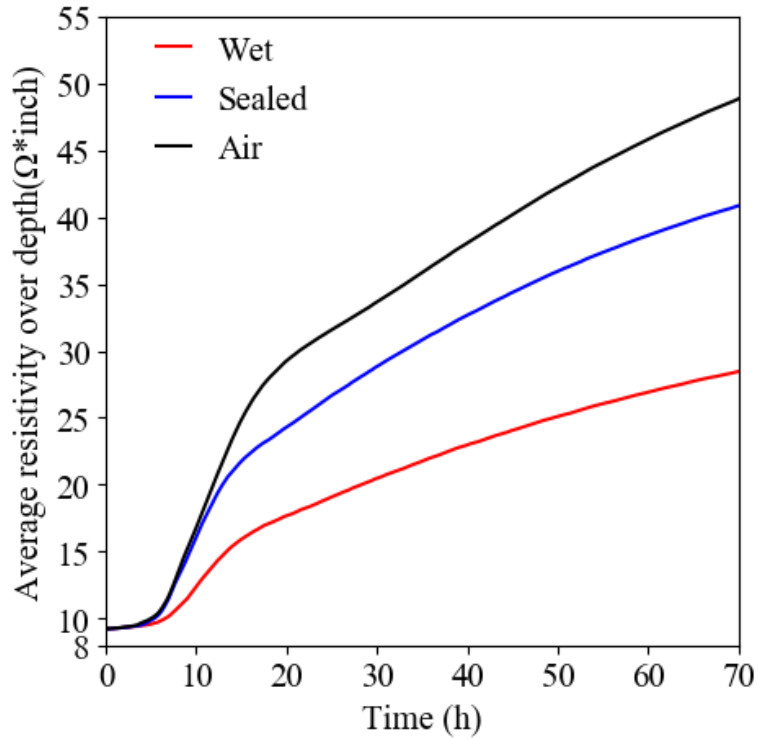
Figure 2-3. Average resistivity curve over the depth of different curing methods.

Figure 2-4 shows the percentage of moisture change for the three curing methods. It shows that the wet curing sample has absorbed moisture within the first 20 h and the air curing sample has the most mass loss in the first 20 h. A slight moisture loss happens to the sealed sample during the first 8 h and then the mass is constant. In all samples, the mass change stopped after roughly 20 h. This is likely caused by the hydration process reducing the porosity and pore connectivity in the mortar. As stated above, the difference in resistivity between curing methods is at least partially caused by moisture differences between the samples. The moisture change curve supports this statement by showing that the air curing sample has the most moisture loss over time and the wet curing sample has moisture absorption over time.
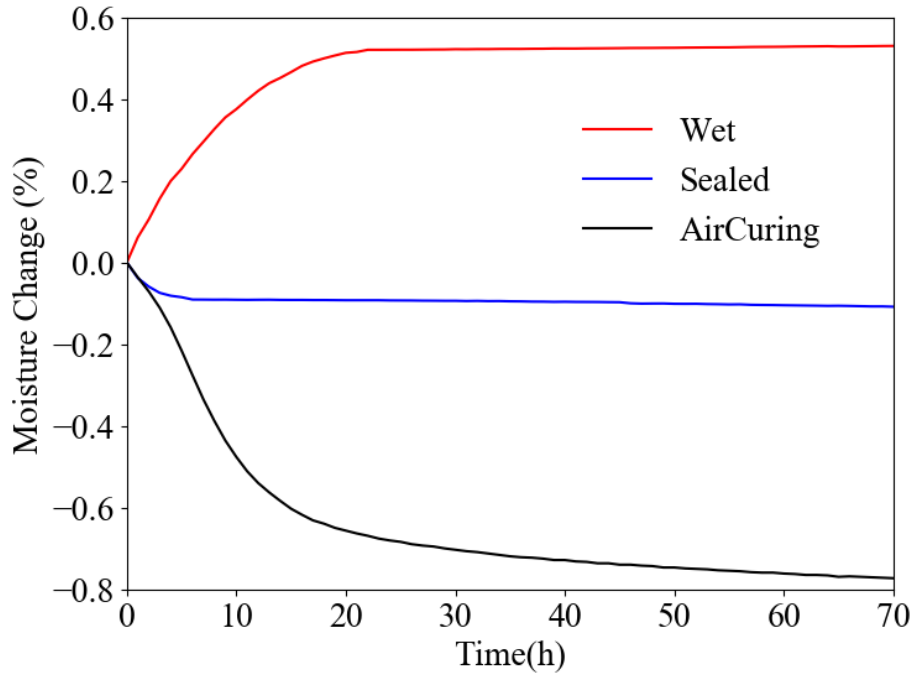
Figure 2-4. Percent moisture change over time.

Figure 2-5 shows the resistivity profile over the sample depth at different times. The wet curing sample had uniform resistivity over the depth. There is a resistivity gradient observed for the air cured and sealed cured samples. This gradient is first observed at about 8 h in the sealed and air cured sample and it continues to magnify over time. These same samples showed measurable moisture loss at 8h in the drying experiments from Figure 4. This loss of water likely contributes to the observed changes in resistivity. The higher resistivity at 0.5 inch compared to 3 inch is expected if there is more moisture loss at the surface of the sample.
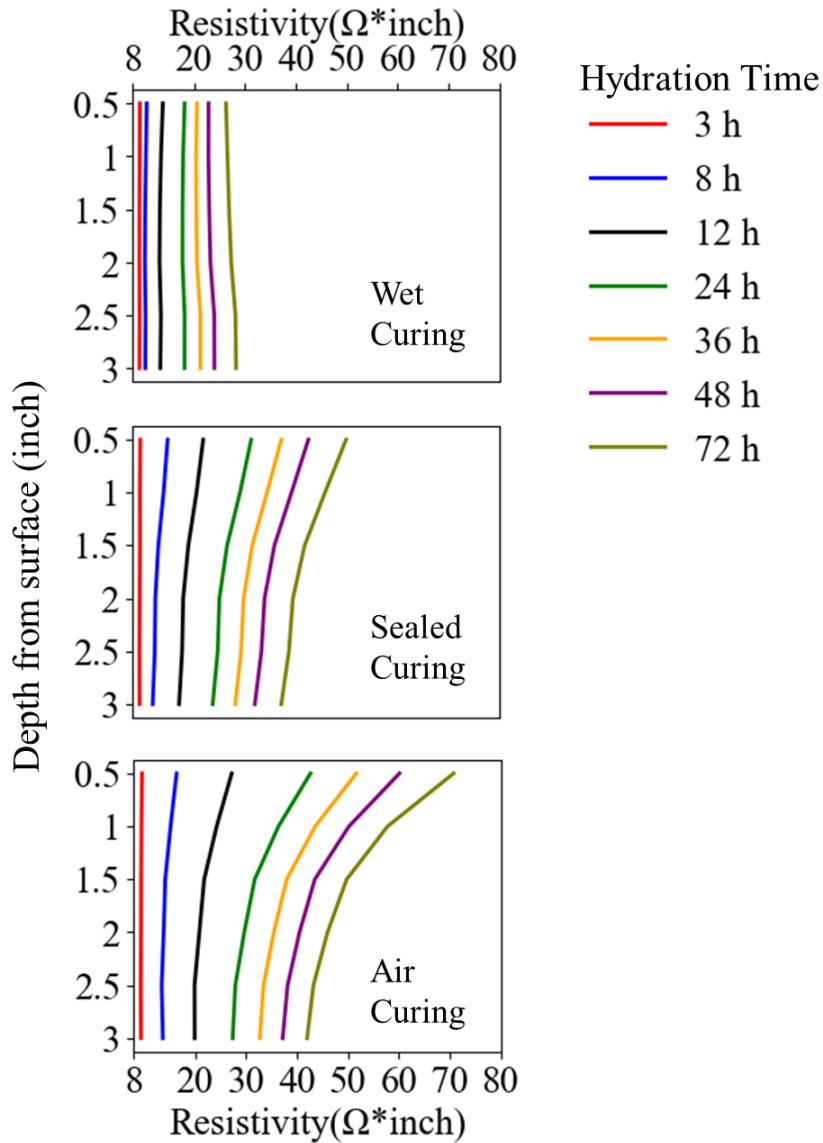
Figure 2-5. Resistivity gradation profile at different time points of wet curing, sealed curing, and air curing

2.3.2 Porosity and DOS change

The DOS of the wet curing specimen is expected to be higher than the other curing methods because of the extra moisture provided over time. Also, this extra moisture promotes the hydration reaction and this will reduce the porosity of the wet curing samples compared to the other methods. For the sealed sample,

the moisture is consumed during the hydration and there is some evaporation over the first several hours of hydration. In the air curing sample, water is consumed during hydration and also lost to evaporation. Because of the loss of water, the air curing sample is expected to have the highest porosity and lowest DOS.

Figure 2-6 shows how the porosity and DOS change over time. Each line on the figure represents a different curing method. At 12h, the three curing methods have almost the same porosity over the depth, which indicates that the degree of hydration of the three curing methods is similar despite the difference in moisture content. It should be noted that after hydrating for 24h, there is a porosity gradient in every sample with the furthest depth having the lowest porosity and the surface have the highest porosity. This higher porosity at the surface may be caused by differences in bleeding. When comparing the results at each depth, the air cured sample has the highest porosity followed by the sealed cured sample and the wet cured sample has the lowest porosity. This difference in porosity between the curing types is caused by the differences in the amount of moisture available for hydration. It should be noted that the air cured sample stopped showing a porosity change at 0.75 inch from the surface after 48 h. This is shown by the green line. This might be caused by the humidity not being high enough within the sample to sustain hydration. More insights into this can be found from the DOS measurements.

The right column of Figure 2-6 shows the DOS or the moisture content within the samples. There is a minimal DOS gradient in the wet cured and sealed cured samples. The sealed cured sample has a lower DOS than the wet cured samples. This difference is caused by the continuous amount of moisture provided on the surface of the wet cured sample. It should be noted that the DOS of the wet curing sample is increasing from 12h to 48h. This is likely caused by the water absorbed into the sample during wet curing. This matches the mass increase observed during wet curing shown in Figure 2-4.

The air cured samples in Figure 2-6 show a lower DOS at all depths compared to the wet and sealed cured samples; however, at 0.75 inch from the surface, the air cured sample shows a much lower DOS than the

wet and sealed cured samples. This lower DOS in the air cured samples is caused by the loss of water from the surface. A direct comparison of the moisture change is shown in Figure 2-4. It should be noted that the DOS for the sample at 0.75 inch depth is below 60% DOS after 48 h for the air cured sample. Based on the previous literature this suggests that hydration should stop when the relative humidity is below 80% [30].
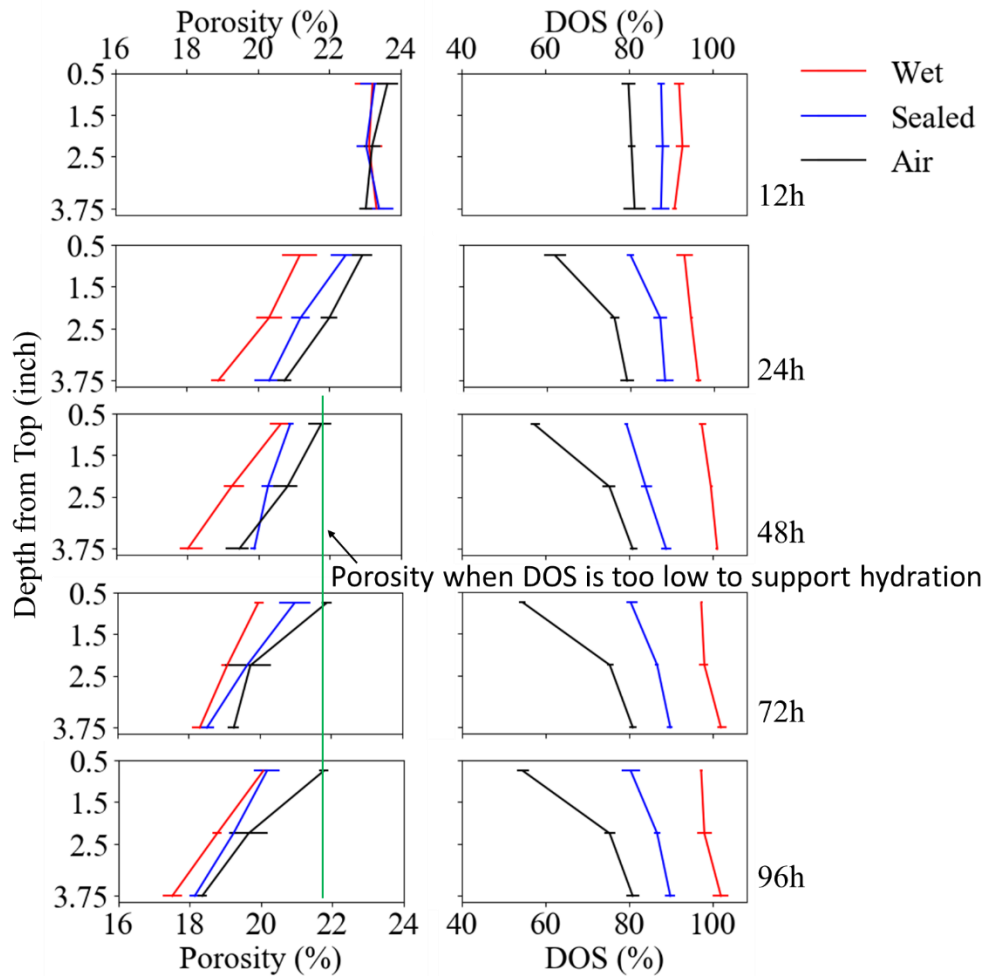
Figure 2-6. Porosity and DOS gradation profile over the sample depth at 12, 24, 48, 72, 96 h of wet, sealed, and air curing.

Figure 2-7 shows the resistivity and DOS at 12, 24, 48, and 72 h of hydration over the sample depth for the three curing methods. The graph shows that the DOS and resistivity curves are correlated. For

16

example, as the DOS begins to decrease, the resistivity increases. This means the resistivity value gives important insights into the moisture content inside the concrete. This also means that a resistivity value taken near the surface and one taken in the depths of the sample could be used as an indicator of the DOS and hence the moisture in the concrete. This could be used as a useful tool to measure the quality of the curing applied to the concrete.
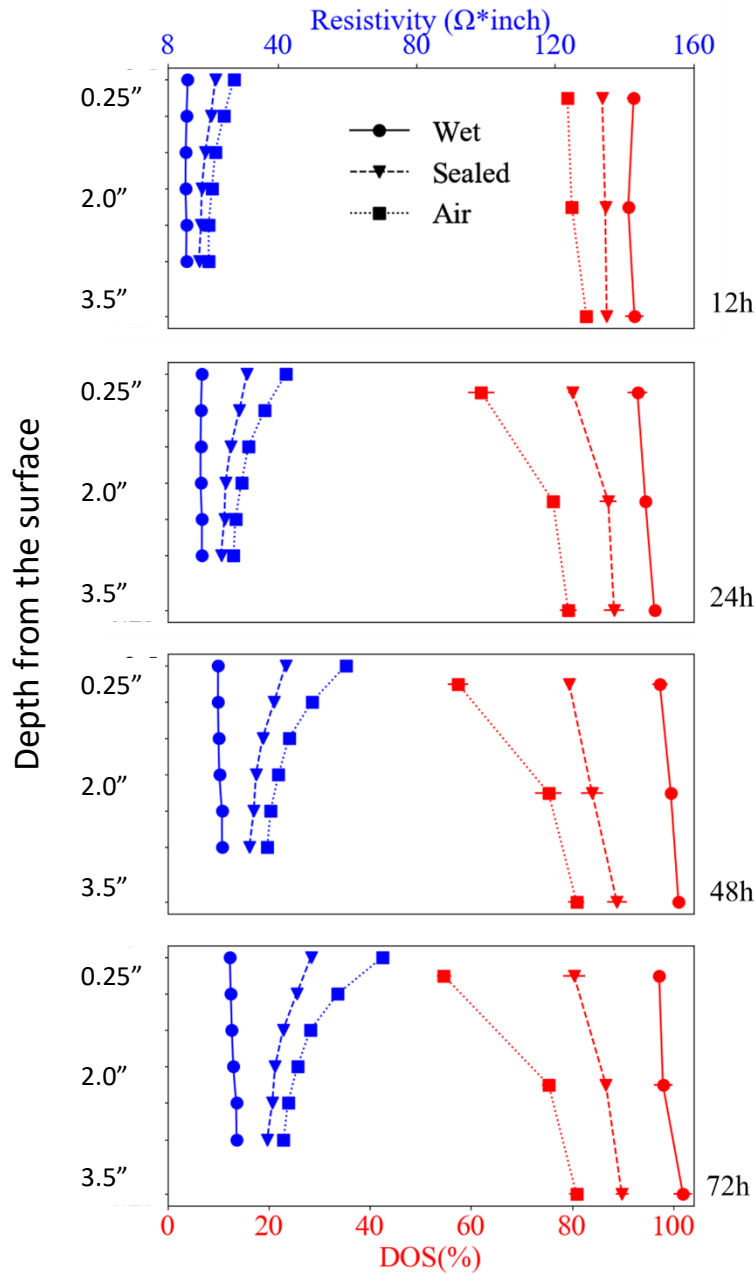
Figure 2-7. Resistivity and DOS at 12, 24, 48, 72 h of hydration of wet curing, sealed curing, and air curing.

Figure 2-8 shows that the resistivity and DOS can be assumed to be linearly related between 12 h and 72 h of hydration. The fitted curve between resistivity and DOS through linear regression at different times

is shown in Figure 2-8. The resistivity at each point was determined by linear interpolation of the two

adjacent points that varied by +/- 0.2 inch.

Figure 2-8 shows that the resistivity and DOS are linearly related between 12 h and 72 h of hydration.

The fitted curve between resistivity and DOS through linear regression at different times is shown in

Figure 8 and this linear regression function can be used to predict the DOS value with resistivity

measurements. The parameters of each fitted line are shown in Table 2-1 in Appendix C. The R square

value is close to 1 for 24h, 48h, and 72h, which illustrates the high accuracy of the linear relationship.

These fitted curves can then be used to predict the DOS at any depth within the sample at a given time.
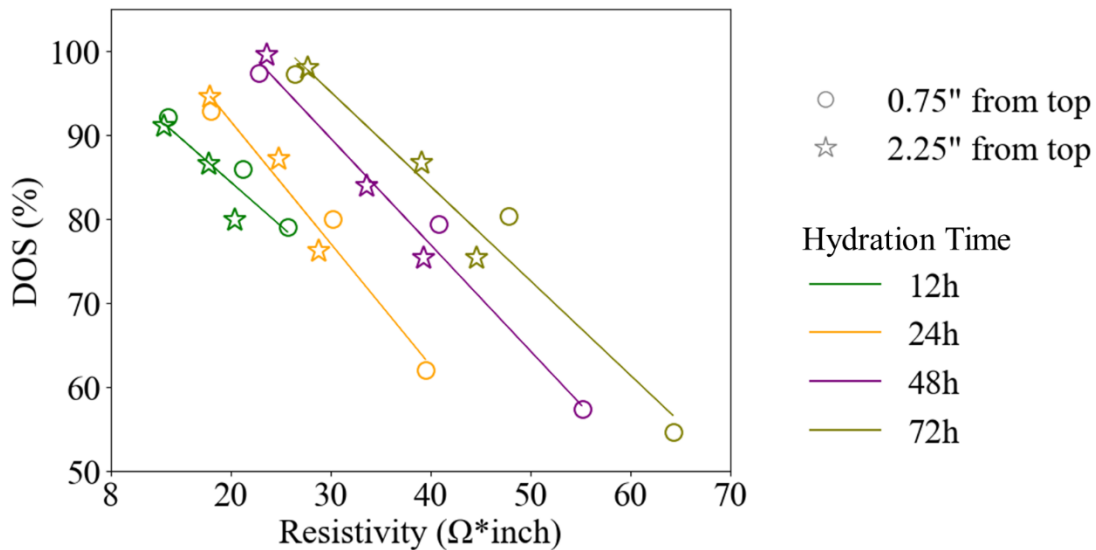
Figure 2-8. DOS is shown as a function of resistivity at 0.75 inch and 2.25 inch from the surface after hydrating for 12, 24, 48, 72h respectively.

Figure 2-9 shows the predicted DOS based on the resistivity measurements. The predicted DOS shows

good agreement with the measured DOS value. This means using resistivity measurement can

quantitatively compare the DOS created by different curing methods for a given set of materials. This can

be used as a new tool to measure how water loss from hydration or drying correlate to the DOS or water

content within a concrete sample. Since this moisture content during hydration is so important to the

properties of the concrete, these resistivity measurements can provide important insights into the material properties of the concrete.
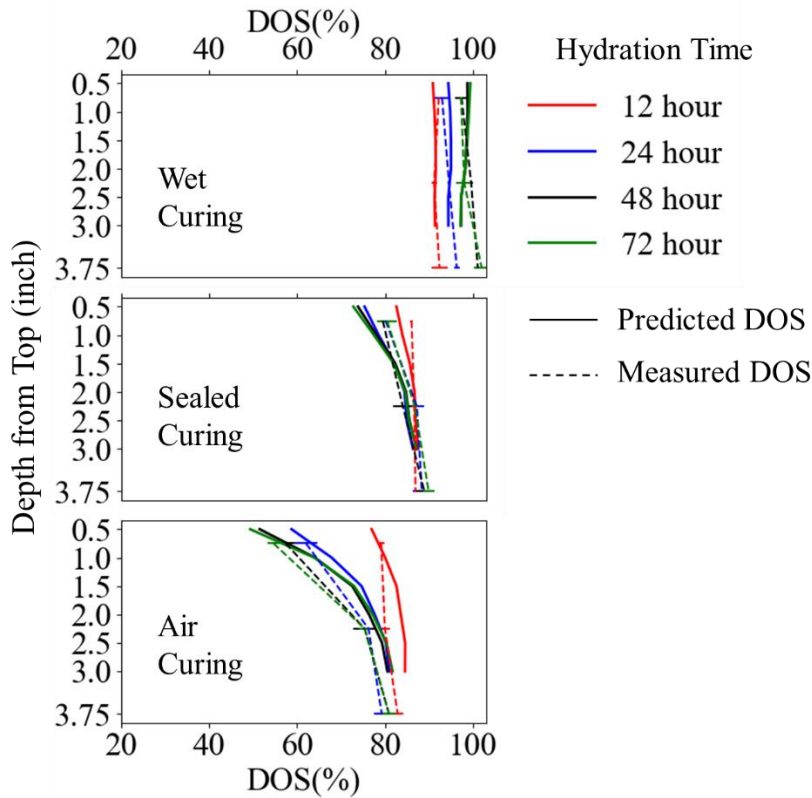
Figure 2-9. Predicted DOS from resistivity at 12, 24, 48, 72 h of hydration compared with the measured DOS.

It can be noted in Figure 2-8 that as the hydration proceeds, the DOS versus the resistivity curve shifts to the right, the slope of the curve decreases, which indicates that resistivity becomes more and more sensitive to DOS change as hydration proceeds. This is likely because the formation of hydration products decreases the porosity and increases the resistance of electron mobility. Figure 2-10 shows the measured porosity versus the resistivity at 86% DOS at different hydration times. This porosity and resistivity were chosen from the sealed curing specimen and a DOS of 86% was chosen because it would ensure

20

hydration is continuing. Because a constant DOS is used, the plot shows how the porosity would change with resistivity at a fixed DOS. This means that as the hydration reaction proceeds, the porosity decreases, and the resistivity increases. The relationship seems to be bilinear between 12 h and 72 h. This change in the shape of the curve could be caused by differences in pore solution chemistry or the connectivity of the pore structure at different times. These are areas of future research. This is an important finding because it shows the ability of resistivity to give insights into the pore structure properties of mortar as it hydrates.
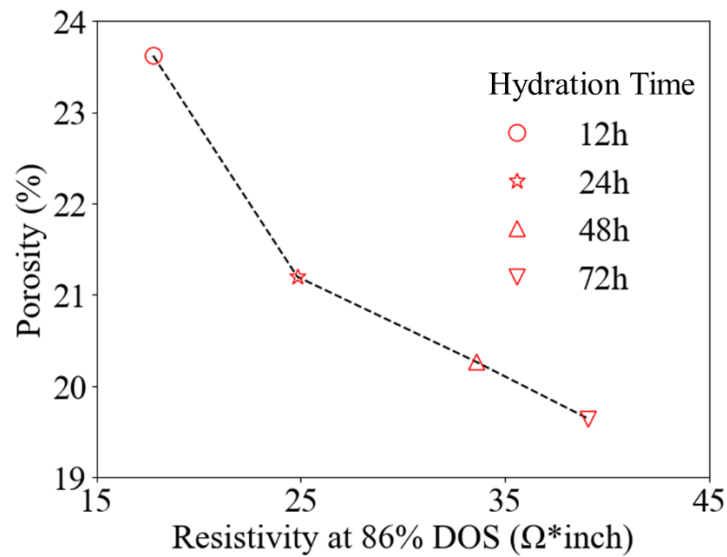
Figure 2-10. The relationship between porosity and resistivity at 86% DOS.

2.3.3 Splitting tensile strength

Figure 2-11 shows the splitting tensile strength at 72 h for the three different curing methods in comparison to the average resistivity at the same time and the same depth. The results show that the resistivity is inversely proportional to the splitting tensile strength of the concrete. For example, the wet curing sample exhibited the highest splitting tensile strength and the lowest resistivity and the air cured sample showed the lowest splitting tensile strength and the highest resistivity. These differences in

strength and resistivity are likely caused by differences in the DOS during hydration. This means that under certain conditions the resistivity can give insights into the tensile strength of the concrete. This is not surprising as Figures 2-8 and 2-10 shows that the resistivity can be related to both the porosity and DOS during the first 72 h of hydration.
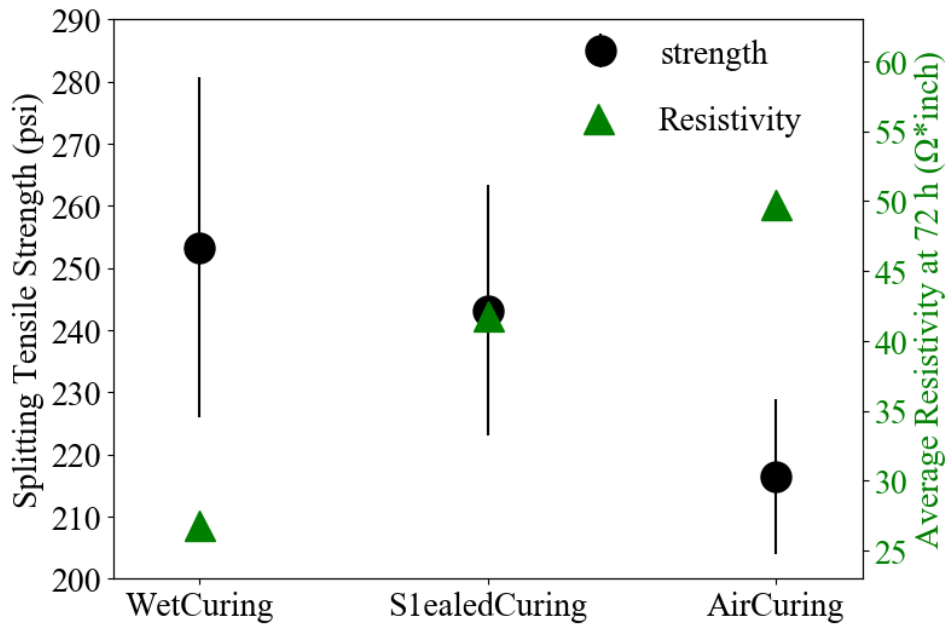
Figure 2-11. Splitting tensile strength at 72 h and average resistivity along depth at 72 h of the three curing methods

2.4 Practical Significance

This work compares the resistivity of air, sealed, and wet curing at different depths in a sample. The results suggest that the resistivity can be correlated to the DOS, porosity, and tensile strength of the sample between 12h and 72h. This means that resistivity measurements during this period could be used to determine the uniformity and effectiveness of different curing methods and provide insights into the uniformity of the hydration over the depth of the sample. This information can provide insights into the porosity and ultimately the strength of the samples at different depths by making real time measurements that are minimally intrusive. These measurements could be used in either the field or the lab to

inexpensively evaluate concrete quality in almost real time. For example, this technique could be used to determine how sensitive a concrete mixture is to different curing practices. This technique could also be used in the field to use the resistivity gradient in the concrete to give insights into the quality of the real time curing and hydration of the concrete. Since the resistivity measurements can be made easily and economically then this makes the measurements very useful.

2.5 Conclusion

A new technique of comparing curing effects using electrical resistivity at different depths was investigated in this study. The electrical resistivity was compared between wet curing, sealed curing, and air curing methods, at different depths within the sample and at different hydration times. These measurements are compared to the porosity, DOS, and tensile strength of the sample, and a linear relationship between resistivity and DOS is created for these materials. The following conclusions can be drawn for mortar between 12h and 72h:

- Resistivity corresponds to the degree of saturation, porosity, and tensile strength for a mortar mixture.
- A linear relationship is developed between resistivity and degree of saturation and this relationship changes as hydration proceeds.
- A bi-linear relationship exists between resistivity and porosity at a fixed DOS that is high enough to promote hydration.
- Wet curing samples showed uniform moisture gradients and had the highest degree of saturation and tensile strength of the samples measured. These samples also showed a 0.5% increase in the mass over the first 20 h of hydration.
- The air cured sample at 73°F and 50% relative humidity environment showed a significant drying gradient over the top 3.35 inch and the refinement of the pore structure stopped after 48 h. This sample also showed a 0.78% decrease in the mass over the first 70 h of hydration.

- The sealed sample showed a uniform moisture gradient and had a degree of saturation, porosity, and tensile strength that is between the wet cured and air cured samples. This sample showed only a slight change in mass during hydration that is likely from an imperfect seal.

- A porosity gradient was observed in all the mixtures regardless of the curing method used. This gradient is likely caused by differences in curing and also bleeding.

This work establishes a systematic method to use resistivity to rapidly and economically measure the in situ degree of saturation, porosity, and provide insights into the tensile strength of the concrete. This could provide a useful scientific and practical measurement technique for future work.

References

[1] Neville, A. M. (1995). Properties of concrete (Vol. 4). London: Longman.

[2] Safiuddin, M., Raman, S. N., & Zain, M. F. M. (2007). Effect of different curing methods on the properties of microsilica concrete. Australian Journal of Basic and Applied Sciences, 1(2), 87-95.

[3] Gowripalan, N. (1990). Effect of curing on durability. Concrete International, 12(2), 47-54.

[4] Zhutovsky, S., & Kovler, K. (2012). Effect of internal curing on durability-related properties of high performance concrete. Cement and concrete research, 42(1), 20-26.

[5] Kosmatka, S. H., Kerkhoff, B., & Panarese, W. C. (2002). Design and control of concrete mixtures (Vol. 5420, pp. 60077-1083). Skokie, IL: Portland Cement Association.

[6] Ramezanianpour, A. A., & Malhotra, V. M. (1995). Effect of curing on the compressive strength, resistance to chloride-ion penetration and porosity of concretes incorporating slag, fly ash or silica fume. Cement and concrete composites, 17(2), 125-133.

[7] Montgomery, F. R., Basheer, P. A. M., & Long, A. E. (1992). Influence of curing conditions on the durability related properties of near surface concrete and cement mortars. Special Publication, 131, 127-138.

[8] Zain, M. F. M., & Matsufuji, Y. (1997). The influence of curing methods on the physical properties of high strength concrete exposed to medium temperature (20–50 ℃). In the Proceedings of the Fifth International Conference on Concrete Engineering and Technology, Kuala Lumpur, Malaysia.

[9] Zain, M. F. M., Safiuddin, M., & Yusof, K. M. (2000). Influence of Different Curing Conditions on Strength and Durability of High-Performance Concrete. ACI SPECIAL PUBLICATIONS, 193, 275-292.

[10] Hajibabaee, A., Moradllo, M. K., Behravan, A., & Ley, M. T. (2018). Quantitative measurements of curing methods for concrete bridge decks. Construction and Building Materials, 162, 306-313.

[11] Hajibabaee, A., & Ley, M. T. (2015). Impact of Wet and Sealed Curing on Curling in Cement Paste Beams from Drying Shrinkage. ACI Materials Journal, 112(1).

[12] Mainguy, M., Coussy, O., & Baroghel-Bouny, V. (2001). Role of air pressure in drying of weakly permeable materials. Journal of engineering mechanics, 127(6), 582-592.

[13] Christensen, B. J., Coverdale, T., Olson, R. A., Ford, S. J., Garboczi, E. J., Jennings, H. M., & Mason, T. O. (1994). Impedance spectroscopy of hydrating cement‐based materials: measurement, Interpretation, and application. Journal of the American Ceramic Society, 77(11), 2789-2804.

[14] Gu, P., Xie, P., Beaudoin, J. J., & Brousseau, R. (1993). AC impedance spectroscopy (II): Microstructural characterization of hydrating cement-silica fume systems. Cement and Concrete Research, 23(1), 157-168.

[15] McCarter, W. J., & Afshar, A. B. (1988). Monitoring the early hydration mechanisms of hydraulic cement. Journal of materials science, 23(2), 488-496.

[16] Li, Z., Wei, X., & Li, W. (2003). Preliminary interpretation of Portland cement hydration process using resistivity measurements. Materials Journal, 100(3), 253-257.

[17] Xiao, L. (2007). Interpretation of hydration process of concrete based on electrical resistivity measurement, PhD Thesis, Hong Kong University of Science and Technology, Hong Kong.

[18] Ghoddousi, P., & Saadabadi, L. A. (2017). Study on hydration products by electrical resistivity for self-compacting concrete with silica fume and metakaolin. Construction and Building Materials, 154, 219-228.

[19] McLachlan, D. S., Blaszkiewicz, M., & Newnham, R. E. (1990). Electrical resistivity of composites. Journal of the American Ceramic Society, 73(8), 2187-2203.

[20] McLachlan, D. S., Rosenbaum, R., Albers, A., Eytan, G., Grammatica, N., Hurvits, G., ... & Zaken, E. (1993). The temperature and volume fraction dependence of the resistivity of granular Al-Ge near the percolation threshold. Journal of Physics: Condensed Matter, 5(27), 4829.

[21] Zhang, J., & Li, Z. (2009). Application of GEM equation in microstructure characterization of cement-based materials. Journal of materials in civil engineering, 21(11), 648-656.

[22] ASTM, C305 (2014). Standard practice for mechanical mixing of hydraulic cement pastes and mortars of plastic consistency. ASTM West Conshohocken, PA.

[23] Tazawa, E. I., Miyazawa, S., & Kasai, T. (1995). Chemical shrinkage and autogenous shrinkage of hydrating cement paste. Cement and concrete research, 25(2), 288-292.

[24] ASTM, C642. (2013). Standard test method for density, absorption, and voids in hardened concrete. ASTM International, West Conshohocken, PA.

[25] T.C. Powers, A discussion of cement hydration in relation to the curing of concrete, Proc. Highw. Res. Board 27 (1947) 178–188.

[26] L.E. Copeland, R.H. Bragg, Self-desiccation in portland cement pastes, ASTM Bull. 24 (February 1955) 34–35.

[27] L.J. Parrott, Load-induced dimensional changes of hardened cement paste, PhD Dissertation, University of London, 1973.

[28] R.G. Patel, D.C. Killoh, L.J. Parrott, W.A. Gutteridge, Influence of curing at different relative humidities upon compound reactions and porosity in Portland cement paste, Mater. Struct. 21 (1988) 192–197.

[29] V. Baroghel-Bouny, P. Mounanga, A. Khelidj, A. Loukili, N. Rafai, Autogenous deformations of cement pastes Part II. W/C effects, micro–macro correlations, and threshold values, Cem. Concr. Res. 36 (2006) 123–136.

[30] Flatt, R. J., Scherer, G. W., & Bullard, J. W. (2011). Why alite stops hydrating below 80% relative humidity. Cement and Concrete Research, 41(9), 987-992.

[31] Robertson, B., McArtor, E., Dickey, M., Ley, MT., Cook, D. (2020) "Development of Concrete Mixtures to Mitigate Bridge Deck Cracking," Oklahoma Department of Transportation (ODOT). ODOT SP&R Item Number 2274. Final Report. Oklahoma City, OK.

[32] Dickey, M. (2021) "Additives to Improve the Performance of Concrete", Thesis requirements for the degree of Master of Science, School of Civil and Environmental Engineering, Oklahoma State University at Stillwater, OK.

CHAPTER 3: Early age hydration investigation on concrete with wet curing at different times

3.1 Introduction

Curing is an important process in producing durable concrete. Wet curing is often used when concrete needs to be the most resistant to deterioration. The purpose of wet curing is to provide continuous moisture to the fresh cement-based system to promote hydration [1, 2]. As a result, wet curing can improve the porosity, permeability, strength, shrinkage and creep of the resulting concrete [3-10]. While there are many benefits with applying wet curing to concrete, there are also challenges because it is labor intensive and can therefore it can challenging to apply the wet curing in a timely manner.

The goal of this work is to investigate the influence of wet curing applied at different times in different evaporative environments to determine the allowable delay in applying the wet curing on the surface before the properties of the concrete are compromised. This work examines the performance in evaporation rates between 0.03 lbs/ft^2/h and 0.17 lbs/ft^2/h. These evaporation rates are commonly observed in practice but are not the highest evaporation rates that can be measured. This research purposely focused on lower evaporation rates as they would show the most potential to delay the application of wet curing. A nomograph predicting the evaporation rates based on different weather conditions is shown in Figure 3-1. The evaporation rates investigated are shown.
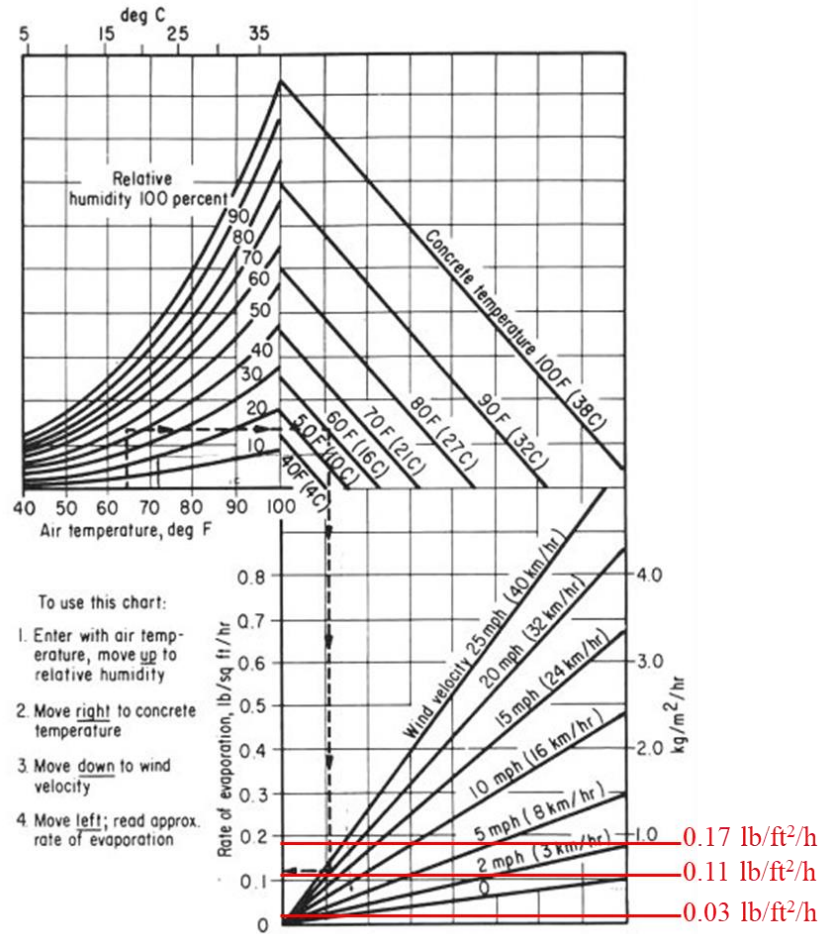
Figure 3-1. ACI nomograph for estimating surface water evaporation rate of concrete i e. the "ACI Hot Weather Concreting Evaporation Nomograph" [11]

The curing methods evaluated include wet curing applied to the surface with no delay or continuous wet curing, wet curing applied with a delay between 2h and 10h, and samples with no curing applied to the surface or air curing. When wet curing is applied to the surface with no delay it will be called "continuous wet curing". The samples that were not cured will be called "air curing".

The impact of these different curing methods are measured by the diffusion coefficient, porosity and degree of saturation (DOS) [18] after 72h of hydration. The resistivity along the sample depth was also used to monitor the hydration for the first 72h, as resistivity measurement is

sensitive, effective, nondestructive, and it can perform rapid and continuous measurement with low cost [12-17]. In addition, the temperature gradient of the samples with the highest evaporation rate (0.17 lbs./ft^2/h) are also measured.

3.2 Experimental Methods

3.2.1 Materials and mixtures

The concrete mixture in this study was prepared according to ASTM C305 [19] with a w/cm ratio of 0.45. The mixture proportion by volume is shown in Table 3-1. The cement used in this study met the requirements of an ASTM C150 Type I Portland cement. The fine and coarse aggregate used for the mixture are locally aggregates that meet the requirements of ASTM C33. The Blaine of the cement is 3560 cm^2/g and the free lime content is 1.4%. The chemical compositions of the cement are shown in Table 3-2. This mortar mixture is designed to be the mortar portion of the concrete mixture used in the other tests in the paper.

Table 3-1. Mixture proportion of concrete

w/cm	Cement (lb/ft^3)	Coarse Aggregate (lb/ft^3)	Fine Aggregate (lb/ft^3)	Water (lb/ft^3)
0.45	22.9	67.3	46.7	8.9

Table 3-2. Chemical composition of cement

	SiO$_2$	Al$_2$O$_3$	Fe$_2$O$_3$	CaO	MgO	SO$_3$	Na$_2$O	K$_2$O	C$_3$S	C$_2$S	C$_3$A	C$_4$AF	LOI
Cement (%)	21.1	4.8	3.1	64.5	2.33	3.2	0.17	0.58	50	23	7	9	2.6

Table 3-3. Mixture proportion of mortar

w/cm	Cement (lb/ft^3)	Fine Aggregate (lb/ft^3)	Water (lb/ft^3)
0.45	37.3	93.3	16.7

3.2.2 Testing Enviornments

The concrete samples were tested under three different environments as summarized in Table 3-4. The 0.03 and 0.11 lb/ft^2/h evaporation rates were obtained by storing the samples at 50% RH and at 73ºF and 100ºF respectively. The highest evaporation rate was obtained by storing the concrete 12 inch away from a 250 Watt heating lamp. A hygrochron sensor showed that the air temperature was 110ºF with a 12% RH. When wet curing was applied, three layers of water-soaked burlap were placed on the surface and then this was sealed with aluminum tape to prevent evaporation. Every day the burlap was removed and soaked with water and placed on top of the sample. The air curing sample was open to the environment.

Table 3-4. Curing methods applied on the concrete samples in different environments

Environments	Maximum Evaporation Rate	Temperature & Humidity	Curing methods applied to concrete samples
Low Evaporation	0.03 lb/ft^2/h	73°F+50% RH	Air curing; Continuous wet curing; Wet curing after exposed in the environment for 3h, 6h, 9h respectively
Middle Evaporation	0.11 lb/ft^2/h	100°F+50% RH	Air cuing; Continuous wet curing; Wet curing after exposed in the environment for 3h, 6h, 9h respectively
High Evaporation	0.17 lb/ft^2/h	110°F+12% RH	Air curing; Continuous wet curing; Wet curing after exposed in the environment for 2h, 4h, 6h, 8h, 10h respectively

3.2.3 Concrete Mixing Procedure

Aggregates were collected from outside storage piles and brought into a temperature-controlled room at 73°F for at least 24 hours before mixing. Aggregates were placed in the mixer and spun and a representative sample was taken for a moisture correction. At the time of mixing all aggregate was loaded into the mixer along with approximately two-thirds of the mixing water. This combination was mixed for three minutes to allow the aggregates to approach the saturated surface dry (SSD) condition and ensure that the aggregates were evenly distributed. Next, the cement, fly ash, and the remaining water was added and mixed for three minutes. The resulting

mixture rested for two minutes while the sides of the mixing drum were scraped. After the rest period, the mixer was started and the admixtures were added. If the SRA or fibers were added, then it was added first and allowed to mix for 15 to 30 seconds, and then the water reducer was added. After the admixtures and/or fibers were added, the concrete was mixed for three minutes.

3.2.4 Evaporation rate

The evaporation rate of the three curing environments was determined by measuring the mass change of the concrete sample over time. The evaporation rate was determined according to Equation 1, where r is the evaporation rate, M_i is the initial mass of the sample, M_n is the mass after evaporation, A is the surface area of the sample, t is the elapsed time. The evaporation was determined by integration of evaporation rate over time shown in Equation 2.

$$Evaporation\ rate: r = \frac{M_i - M_n}{A*t} \qquad Equation\ 1.$$

$$Evaporation = \int r\ dt \qquad Equation\ 2.$$

3.2.5 Electrical resistivity

The molds were 6 inch diameter by 9 inch tall plastic cylinders. The cylinders used seven layers of 4-40 threaded stainless steel rods with a 0.18 inch diameter. Each layer used two rods with a horizontal spacing of 3.65 inch and a vertical spacing of 0.5 inch. The steel rods were installed through the molds and were stabilized and sealed with glue before the concrete was placed. The configuration of the specimen is shown in Figure 3-2. Concrete was used to fill the mold to 8 inch in height. The top 1 inch was not filled to allow curing methods to be applied. The concrete was placed in three layers. For each layer, the sample was consolidated for 10 s with a vibrating table at a frequency of 60 Hz to remove entrapped air and to promote a good bond with the threaded rod.

31

During hydration water is consumed and the sample shrinks [20]. This change in volume may form a gap between the mold and the edge of the sample. To ensure that the drying is only from the top of the sample and not from the edges, the edge of the fresh mortar was sealed and covered by mortar. More details can be found in Appendix A.
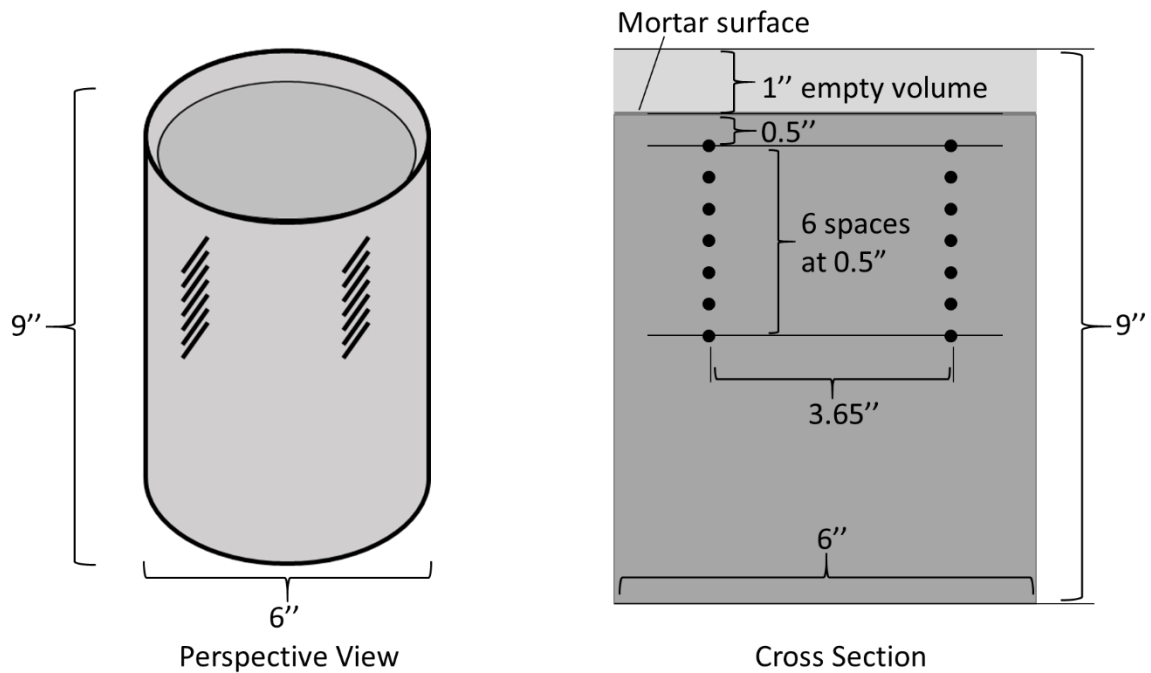
Figure 3-2. Configuration of the mortar sample for resistivity measurement

After the samples were cast into molds, the resistivity was measured between the rods every 10 minutes through the hydration process. The circuit for the resistivity measurement was programmed with the Arduino platform. An Arduino Mega 2560 was used as the central processor with a 12-Bit impedance converter AD5933. In this research, a frequency of 30 KHz was used. The system was calibrated with a 100-ohm resistor. The calibration process was to calculate the Gain Factor of the system based on a known resistor. The Gain Factor can then be used to calculate the resistivity of future measurements. The detailed calculations are in Appendix B.2. Five multiplexers are used to measure 80 channels simultaneously. The results are

recorded on a SD card and retrieved for analysis. More details about the additional hardware and the raw data process of resistivity can be found in the Appendix B.1.

3.2.5.1 Resistivity gradient

The resistivity gradient is calculated along the sample depth from 0.5 inch to 3.5 inch from the sample surface. Equation 3 was used to calculate the resistivity gradient, where $R_{0.5inch}$ and $R_{3.5inch}$ are the resistivity at the depth of 0.5 inch and 3.5 inch from surface measured at the same time of hydration. The gradient is a helpful measurement to compare the resistivity between curing methods because before the application of wet curing, the bottom the of the sample at 3.5 inch is moist and the sample at the surface could be different. By using the resistivity at 3.5 inch this normalizes

$$Resistivity\ gradient = (R_{0.5inch}-R_{3.5inch})\ /\ (89\text{-}13)\ (\Omega*inch\ /\ inch) \qquad Equation\ 3.$$

3.2.6 Temperature

The temperature at different depths was measured on concrete samples in the highest evaporation environment during air curing, continuous wet curing and wet curing after drying for 6h. The concrete samples for temperature measurement were cast into the same molds as those for the resistivity test. Four type T thermocouples were used along the depth as shown in Figure 3-3 before the concrete were filled. The thermocouples were stabilized and sealed by glue. The molds were filled in the same way as that of the resistivity test. The temperature was measured with a time interval of 10 minutes.
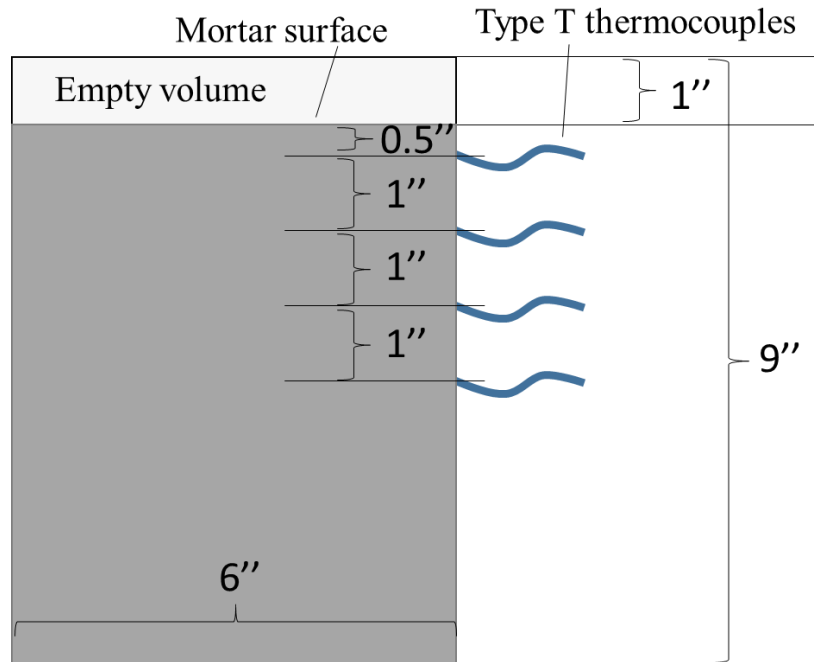
Figure 3-3. Configuration of the thermocouples of the mortar sample

3.2.7 Porosity and degree of saturation (DOS)

The porosity and degree of saturation (DOS) [21] are investigated to examine the curing influence in the three environments by using mortar samples. Mortar samples are used because coarse aggregates can significantly impact the measurements of these tests. The mixture design of mortar samples is shown in Table 3. The mortar samples were cast into tubes with 1 inch diameter by 4.5 inch tall. Each tube was filled with three layers of mortar.

The porosity measurement allows the total pores to be compared between mixtures. As the hydration continues then it is expected that the porosity would decrease. This means that a sample with a higher porosity will have a lower amount of hydration and also lower strength and possibly higher diffusion coefficient.

The DOS shows the amount of moisture within the sample. This allows the relative moisture content of the different samples to be compared when the samples are 72h old. This is useful because the moisture

34

content of the sample is important to understand the diffusion results. Also, the air dried samples provide insight into the amount of drying in the sample and how that impacts hydration. Other research shows that hydration ceases at a relative humidity of about 80% due to negative capillary pressure that opposes the reaction [22], and this is close to a DOS of 65% [23].

The porosity and DOS were measured when the samples were 72h old. For each curing method and time period, three samples were measured. At 72h the sample was demolded and cut into 3 segments that are each 1.5 inch tall. This means that the distance to the midpoint of each segment is 0.75 inch, 2.25 inch, and 3.75 inch from the sample surface. This is helpful to determine the porosity and DOS at different depths.

The porosity and DOS were determined by ASTM C642 with some minor changes where the samples were saturated within a vacuum chamber instead of boiling in water. Equation 4 and 5 were used to calculate the porosity and DOS, where W_i is the initial weighs of the sample, W_d is the oven dried weight at 230 ºF, W_{sa} is the saturated surface dried (SSD) weight, W_{su} is the suspended apparent mass of the saturated samples.

$$DOS = \frac{W_i - W_d}{W_{sa} - W_d} \times 100 \qquad\qquad Equation\ 5.$$

$$Porosity = \frac{W_{sa} - W_d}{W_{sa} - W_{su}} \times 100 \qquad\qquad Equation\ 4.$$

3.2.8 Diffusion coefficient

The mortar mixture used for diffusion testing is the same as the porosity and DOS and is shown in Table 3-3. The containers for the mortar sample were 0.6 inch diameter by 4.47 inch long cylinders. The mortar samples were cured in the same way as the concrete samples. When it was time to wet cure the samples, water was placed on the top. The air cured sample never received water. For each curing method, four samples were measured.

35

The configuration of the diffusion test is shown in Figure 3-4. In this test, the diffusion coefficient of the mortar was obtained by placing KI solution on the sample and monitoring the ion penetration depth over time. This method has been described in previous publications [24-27]. The higher the diffusion coefficient, the easier for the sample to be penetrated by outside chemicals, this makes the concrete more susceptible to damage caused by chlorides or other chemicals.
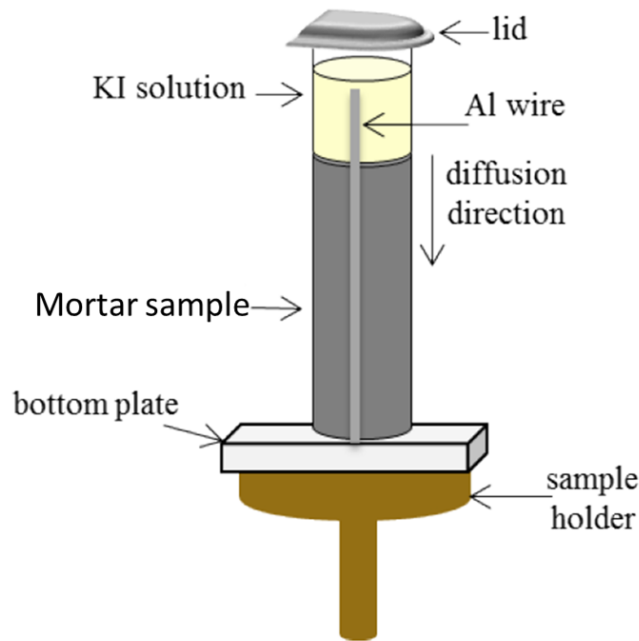
Figure 3-4. Configuration of Diffusion Testing

3.3 Results and Discussion

3.3.1 Evaporation

The total amount of evaporation and the rate of evaporation is shown in Figure 3-5. The maximum evaporation rate will be used for discussion in this paper because a widely available tool exists in Figure 3-1 to calculate this value. Within the first hour of measurement the maximum evaporation rate was measured for each sample. The lowest evaporation rate of 0.03 lb/ft^2/h is for a sample that was stored at 73°F and 50%RH. This sample had an almost constant evaporation rate. The sample stored at 100°F and

50%RH had the next highest evaporation rate at 0.11 lb/ft^2/h. The evaporation rate was constant from the

first measurement until 4h later. The highest evaporation rate is 0.17 lb/ft^2/h. This sample was stored 12

inch away from a 250 Watt heating lamp. This maximum evaporation rate was only held for about 2h and

then decreased. It is interesting that the evaporation rate for the 0.11 and 0.17 lb/ft^2/h sample followed a

very similar trend between 5h and 12h. This could be because both surfaces are predominately solid and

so they have a similar resistance to evaporation. More work is needed to better understand this.
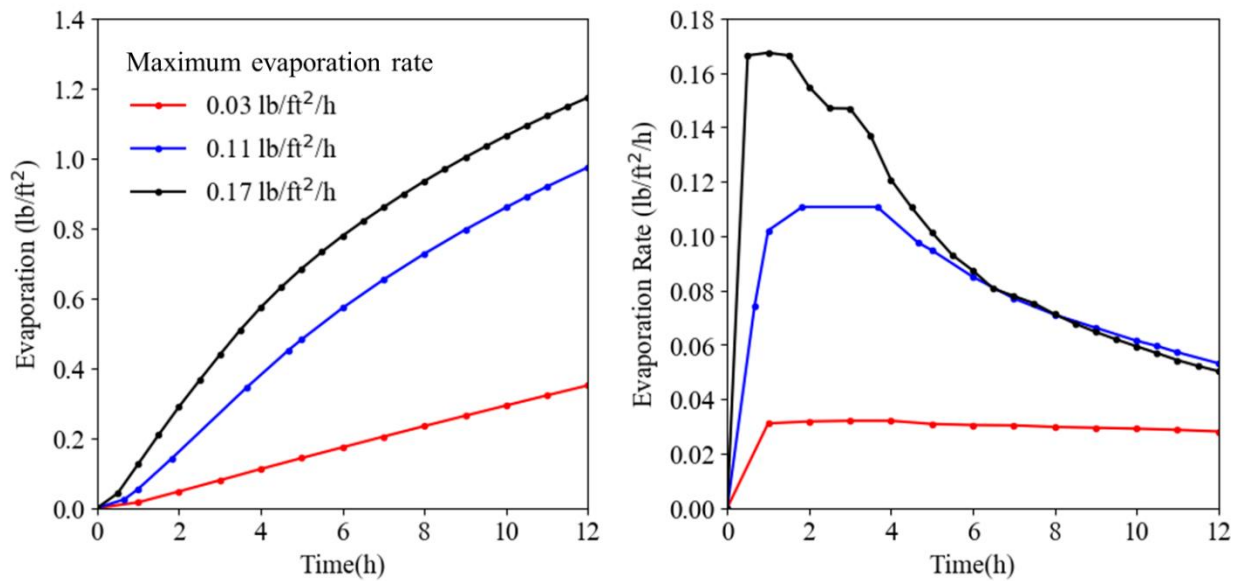
Figure 3-5. (a) Evaporation over time of the three curing environments, (b) Evaporation rate over time of the three curing environments

3.3.2 Temperature

The temperature at different depths within the concrete in the highest drying environment is shown in

Figure 3-6. The results are shown for air curing, continuous wet curing, and wet curing after drying for

6h. Each curve shows the heat from the exothermic reaction of hydration that occurs at roughly 9h. The

results show that the temperatures within the concrete are greatly impacted by how the samples are cured.

The air curing sample had the highest temperature at 0.5 inch from the surface of about 110°F and the

other depths were about 104°F after 10h of hydration. The continuous wet curing had a uniform

37

temperature that was about 59°F less than the air curing sample. The sample initially open to the

environment for the first 6h had a similar temperate as the air curing sample over the first 6h; however,

after the wet burlap was placed on the concrete the temperature dropped to be similar to the sample with

continuous wet curing. This shows that even after 6h of drying, the wet curing can reduce the internal

temperature of the concrete to levels that are similar if it was continually wet cured even in hot and dry

environments. This is useful to understand the internal temperature gradient within the concrete.
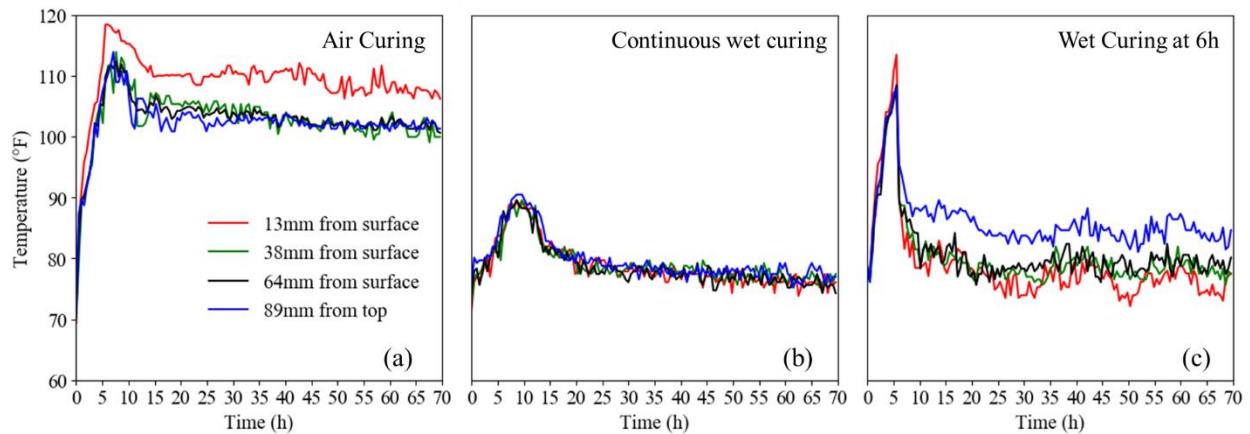
Figure 3-6. Temperature over time inside the concrete samples under the heat lamp of (a) air curing, (b) continuous wet curing, (c) wet curing after drying for 6h.

3.3.3 Electrical resistivity

The average electrical resistivity over the depth of the concrete samples for the three different drying

environments is shown in Figure 3-7. An overview graph is shown as well as a zoomed graph that

provides more details. Note that the reduction in resistivity corresponds with the time when the wet

curing was placed on the sample. There is no correction for differences in temperature in this data as the

impact of temperature is shown to be insignificant because the resistivity is controlled by the DOS of the

sample during this period [23].

In each environment, before the wet curing is applied, the resistivity curve follows the air curing sample. One important observation is that once the wet curing is placed on the samples with the 0.03 and 0.11 lb/ft^2/h evaporation rates, the resistivity matches the concrete that received continuous wet curing. This seems to suggest that even though the samples have been drying in these environments, once the water is placed on the surface the electrical resistivity returns to the same values as if it was continuously wet cured. This seems to indicate that a drying period of 9h in 0.03 and 0.11 lb/ft^2/h evaporation rate did not keep water from penetrating the concrete; however, this is not the case in the 0.17 lb/ft^2/h evaporation rate environment. In this environment, the sample that was drying for 2h returned to the same electrical resistivity level as the sample that had been under continuous wet curing but the sample that was cured for 4h did not. This higher resistivity level after placing the wet curing suggests that the material has been altered by the drying. This suggests that the material has been microcracked or the structure has been altered in a way that the drying has created a permanent change in the material.

Figure 3-7. Electrical resistivity of the concrete in different drying environments for wet curing placed at different times on the surface.

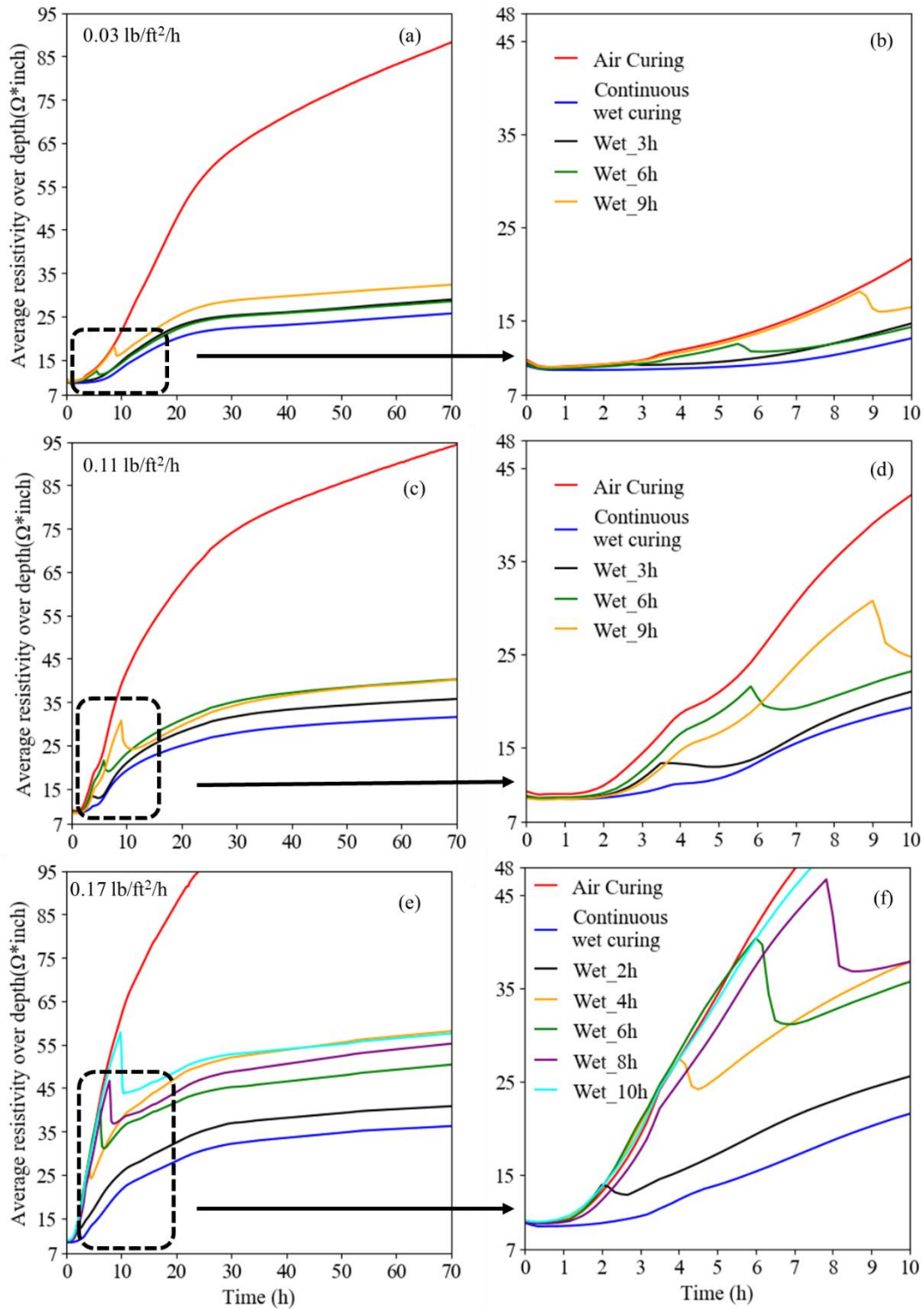### 3.3.4 Porosity and DOS test

In the air curing sample, water is consumed during hydration and is also lost to evaporation. Because of the loss of water, the air curing sample is expected to have the highest porosity and lowest DOS. The DOS of the specimen with wet curing applied is expected to be higher than the air curing sample because of the extra moisture provided over time.

Figure 8 shows how the porosity and DOS change as the wet curing is applied at different times. For all of the evaporation rates the DOS of the wet cured samples at any time period are very similar. Since the DOS measures the amount of water in the pores, this shows that the wet curing filled the available pores at all of the evaporation rates. The DOS of the air cured samples is helpful to understand the severity of the drying that occurs at different depths of the sample. As expected, the relative ranking of the DOS at the surface matches the relative ranking of the maximum evaporation rate. It is interesting to note that all three drying environments showed very similar DOS at 2.4 inch and 4 inch from the surface. This shows that differences in surface drying primarily impacts the top 4 inch of the sample.

The porosity measures the total volume of pores in the sample. Differences in the porosity between the continuously wet cured sample and the others with delayed wet curing shows that there was a change in the amount of hydration that caused more pores in the concrete. These additional pores would lower the strength of the surface concrete and could increase the diffusion coefficient. A reduction in strength would mean the concrete is more likely to crack and have reduced abrasion resistance. The increase diffusion coefficient could reduce the service life of the concrete.

For the 0.03 $lb/ft^2/h$ evaporation rate, there seems to be little difference in the porosity for the continuously wet cured samples and the samples with a delay in wet curing up until 6h. The sample with a delay in wet curing of 9h did show an increase in porosity at 0.8 inch and 2.4 inch from the surface but no difference at 4 inch from the surface. This means that for the evaporation rate of 0.03 $lb/ft^2/h$ that wet

curing could be delayed up until 6h and there is no significant impact on the porosity but there is an impact after 9h of drying.

For the 0.11 lb/ft^2/h evaporation rate, there is no difference for the sample that the wet curing was delayed 3h but there is a measurable difference for the sample where the wet curing was delayed 6h. The sample where the wet curing was delayed 9h showed even higher porosity at the surface. This means for this environment the wet curing could be delayed 3h at the surface without impacting the porosity of the sample.

For the highest evaporation rate of 0.17 lb/ft^2/h, the porosity measurements show that the longer the sample is exposed to the environment, the higher the porosity of the sample at the surface. These measurements also show that the surface porosity is significantly modified after 2h of drying. This means that wet curing would need to be applied earlier than 2h in this drying environment to not impact the porosity of the sample. An estimated safe time can be found with the resistivity gradient.
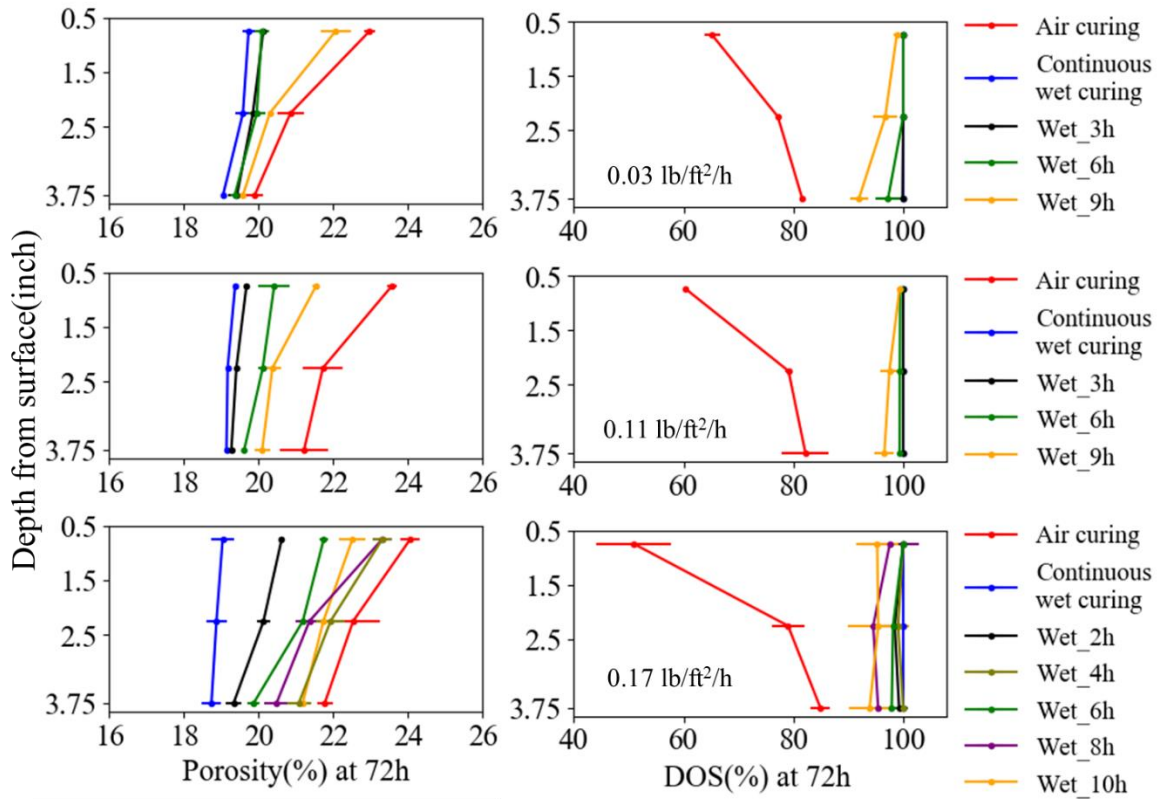
Figure 3-8. Porosity and DOS gradation profile along the sample depth at 72h hydration at different environments.

Because the electrical resistivity measurements are made continuously, they can be compared to the porosity. Further analysis shows that the slope or the gradient of the electrical resistivity measurement correlates to the porosity at 0.8 inch from the surface. These results are shown in Figure 3-9.

For the 0.11 $lb/ft^2/h$ and 0.17 $lb/ft^2/h$ evaporation rates the porosity at 0.8 inch increased with an increase in the resistivity gradient. This increase in gradient means that more water has been lost to the sample. This means the concrete has had less water available for hydration and so this has impacted the porosity. For the 0.03 $lb/ft^2/h$ evaporation rate, there is little difference between the evaporation rate and the porosity for the sample at 3h and 6h.

For both the 0.03 lb/ft^2/h and 0.55 lb/ft^2/h environments, there was a significant difference in the porosity at 6h and 3h respectively. The resistivity gradient at both of these times is 0.3 Ω*inch/inch. This means that this resistivity gradient may be a helpful way to determine the drying time for an allowable porosity limit for the 0.17 lb/ft^2/h drying environment. The resistivity gradient over time is shown in Figure 3-10 for the air cured sample in the 0.17 lb/ft^2/h drying environment. The results show that a resistivity gradient of 0.3 Ω*inch/inch is reached after 1.35 h.
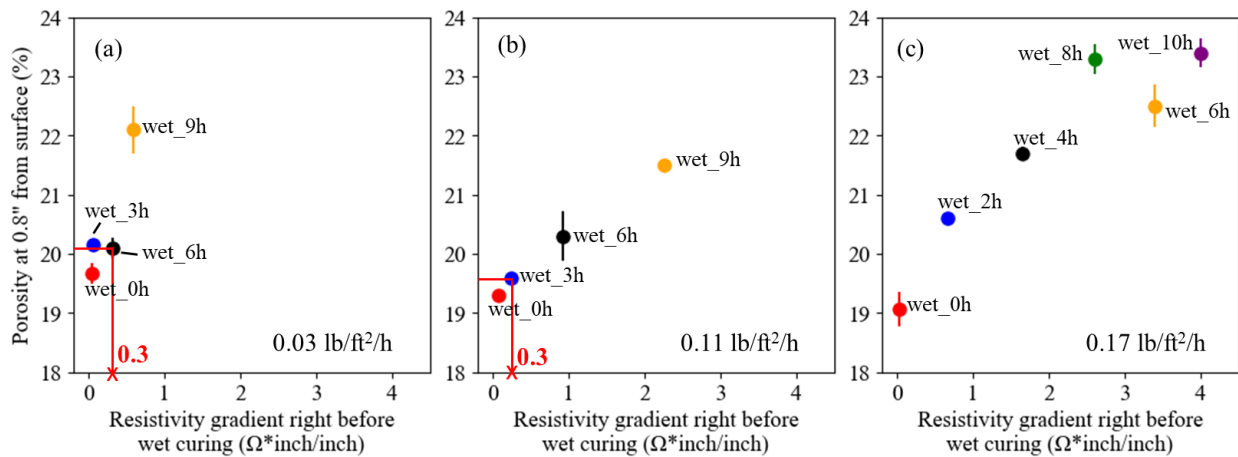
Figure 3-9. Porosity at 0.8" from the surface versus the resistivity gradient right before wet curing is applied for different drying environments.
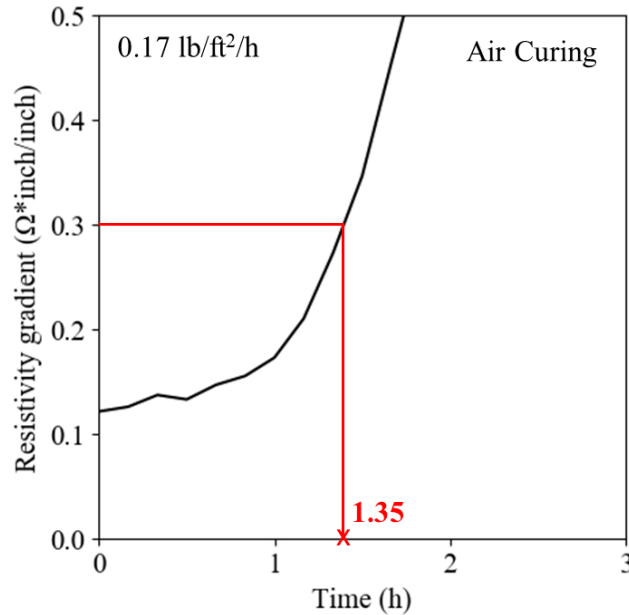
Figure 3-10. Resistivity gradient over time at 0.17 lb/ft2/h evaporation rate environment for the air curing sample.

3.3.5 Diffusion coefficient

The diffusion coefficient for different evaporation rates and curing times is shown in Figure 3-11, and a student t test between continuous wet curing and the other curing methods is shown in Table 3-5 and Table 3-6. In the t test results, if the calculated t value is greater than the theatrical t value (2.447 in this case), the groups are categorized as not similar, otherwise the groups are categorized as similar.

In all cases the continuously wet cured sample performed the best and the air cured sample performed the worst. Also, as the evaporation rate became more severe, the diffusion coefficient increases. As the diffusion coefficient increases this means the resistance to outside chemical penetration also decreases and this decrease the durability of the concrete.

All the samples cured in the lowest evaporation rate (0.03 lb/ft^2/h) seem to have a similar diffusion coefficient. A student t test was used to show that there is no statistical difference in these measurements.

45

The results are shown in Table 3-5. This means that the drying did not impact the measured diffusion coefficient. In the $lb/ft^2/h$ evaporation rate, all the curing periods have a similar diffusion coefficient except for the air cured sample. It doesn't appear that the diffusion coefficient detects a difference in delaying the curing to be placed on the concrete until at least a 9h delay, and this shows agreement with the t test results. The diffusion coefficient does not seem to be as sensitive to the delay in curing as does the porosity measured in the previous section.

At the highest evaporation rate ($0.17 \ lb/ft^2/h$), the continuously wet cured sample has a higher diffusion coefficient to the other drying environments. This could be caused by the higher temperature impacts the uniformity and quality of the hydration products. Also, when the wet curing is delayed this causes the diffusion coefficient to increase almost linearly with time until 8h. The results also show that even delaying the application of the wet curing by 2h will cause an increase in the diffusion coefficient. The t-test results also show that all the delayed wet curing has a statically different mean as that of the continuously wet cured sample. This shows the importance of placing wet curing on the surface quickly in a high drying environment as a 2h delay will impact the diffusion coefficient.

Care should be taken in evaluating the diffusion coefficient of the air cured samples to the others. The air cured samples will have a lower amount of water in their pores from drying that was never replenished with applied water. When the tracer solution is added to these samples it will be drawn in by a combination of diffusion and absorption. This will make the measured diffusion coefficient to appear to be larger. This doesn't occur in the wet cured samples because the water added to the surface increases the DOS and so the movement of the outside fluid into the concrete would only be caused by diffusion.
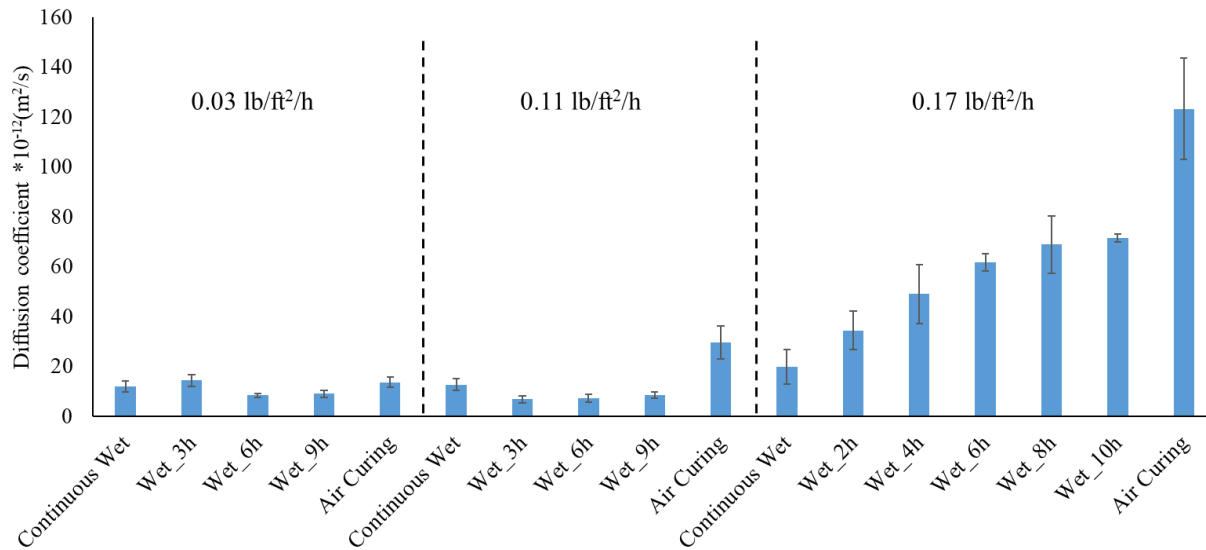
Figure 3-11. Diffusion coefficient of the mortar samples under different curing methods

Table 3-5. Student t test result between continuous wet curing and the other curing methods in different environments on diffusion coefficient at 0.03 and 0.11 lbs/ft²/hr.

	Wet_3h	Wet_6h	Wet_9h	Air Curing
Continuous Wet @ 0.03 lb/ft²/hr	1.46, similar	1.03, similar	0.75, similar	1.06, similar
Continuous Wet @ 0.11 lb/ft²/hr	2.35, similar	2.4, similar	1.66, similar	4.87, not similar

Table 3-6. Student t test result between continuous wet curing and the other curing methods in different environments on diffusion coefficient 0.17 lbs/ft²/hr.

	Wet_2h	Wet_4h	Wet_6h	Wet_8h	Wet_10h	Air Curing
Continuous Wet @ 0.17 lb/ft²/hr	2.87, not similar	4.27, not similar	10.93, not similar	7.34, not similar	14.55, not similar	9.63, not similar

Note: 1. The t test hypothesis is that: the two group means is the same.

Note 2. Parameters for the t test: significance value $\alpha = 0.05$; degree of freedom = 6; theoretical

t value = 2.447.

3.3.6 Practical Significance

This work compares the resistivity, diffusion coefficient, porosity and DOS of wet curing at different times and air curing on concrete and mortar samples. The results show that the critical timing for applying wet curing is based on the evaporation rate of the concrete.

The work also shows that the porosity measurements in this work are more sensitive to changes to early age drying than the diffusion coefficient. Table 3-7 shows the critical time for applying the wet curing to the surface for porosity and diffusion coefficient for the three different drying environments investigated.

Table 3-7. Allowable delay in wet curing before performance is compromised.

Maximum Evaporation Rate	Porosity	Diffusion Coefficient
0.03 lb/ft^2/h	6h	>9h
0.11 lb/ft^2/h	3h	9h
0.17 lb/ft^2/h	1.35h*	<2h

*Note: this is determined from electrical resistivity measurements.

This shows that in the least severe drying environment of 0.03 lb/ft^2/h evaporation rate, the wet curing can be delayed for 6h and there will be no statistically significant change in the porosity or diffusion coefficient. When the drying rate is increased to 0.11 lb/ft^2/h, wet curing can be delayed for 3h before there is statistically significant change in the porosity or diffusion coefficient. For the highest rate of evaporation of 0.17 lb/ft^2/h evaporation rate, the delay must be less than 2h. Based on the gradient measurements from the resistivity testing, the critical time for application of the wet curing is 1.35 h. The reader should be reminded that this table shows the exact time when performance is compromised and that it is typical to use a safety factor for specification requirements. Also, this work only used a single concrete mixture and the testing only examined three different drying environments. For all of these reasons, it is challenging to make a recommended change to the current ODOT specifications. However,

with more measurements and a wider range of materials and drying environments then a recommendation could be made on safe delays in applying wet curing.

There are two possible ways to future implementation of these findings. First, a specification could be used where the evaporation rate in the environment is measured and based on the maximum evaporation rate a certain delay is allowed in applying the curing to the concrete. Hand held weather stations already exist that could do this by measuring all of the variables and the nomograph from Figure 1. However, there has been some question about the validity of the nomograph and also criticism that the recommendations of the nomograph do not depend on the type or quality of the concrete.

Another option would be to measure the resistivity gradient in the field of the fresh concrete. This measurement would capture the difference in moisture loss between the top and bottom of the sample. This would allow you to measure the impact of the environment on the concrete while taking into account the bleeding rate of the concrete. For this to be a practical approach, work needs to be done to understand what resistivity gradient is allowable before the properties of the material are compromised.

It is also important to note that this work suggested the allowable limits based on the changes in the porosity. It is not clear how these changes would relate to a loss in other physical properties like abrasion resistance or strength. It should also be noted that the measured diffusion coefficient was as sensitive as the porosity measurement. More measurements would provide greater insights to when a critical property is being impacted from the delay in the wet curing.

3.4 Conclusion

The influence of wet curing at different times was investigated in this study. The experiments were conducted under three different evaporation conditions for the first 72h of hydration. The diffusion coefficient, porosity, DOS, and resistivity of the sample were measured and compared between curing methods. The following conclusions can be drawn:

49

- The electrical resistivity measurements are able to show the loss in moisture over time in all three drying environments. When wet curing was applied to the surface after 9h of drying for the samples in the 0.03 lb/ft^2/h and 0.11 lb/ft^2/h evaporation rate, the resistivity decreased to values similar to of the sample was never allowed to dry. However, in the 0.17 lb/ft^2/h evaporation rate for at least 2h, the resistivity did not decrease to the same level as the sample continuously wet cured.

- At the 0.03 lb/ft^2/h evaporation rate environment, delaying the wet curing for 6h did not impact the porosity of the sample. The diffusion coefficient was not impacted when the wet curing was delayed for 9h.

- At the 0.11 lb/ft^2/h evaporation rate environment, delaying the wet curing for 3h did not impact the porosity of the sample. The diffusion coefficient was not impacted until the wet curing was delayed for 9h.

- The average porosity at 0.8 inch in depth is related to the resistivity gradient right before the application of curing in the 0.11 lb/ft^2/h and 0.17 lb/ft^2/h evaporation rate. The resistivity gradient was also useful in predicting the change in the diffusion coefficient in the 0.17 lb/ft^2/h evaporation rate. This shows that the resistivity gradient in the sample during curing could be used to track changes in the surface porosity and the diffusion coefficient from drying.

This work would benefit from additional testing done in the field to verify the measurements and also to compare the predicted performance with a wider range of materials; however, the results show promise for establishing a method to measure the impacts of delaying wet curing in different environments on the porosity and diffusion coefficient of concrete.

References

[1] Neville, A. M. (1995). Properties of concrete (Vol. 4). London: Longman.

[2] Safiuddin, M., Raman, S. N., & Zain, M. F. M. (2007). Effect of different curing methods on the properties of microsilica concrete. Australian Journal of Basic and Applied Sciences, 1(2), 87-95.

[3] Gowripalan, N. (1990). Effect of curing on durability. Concrete International, 12(2), 47-54.

[4] Zhutovsky, S., & Kovler, K. (2012). Effect of internal curing on durability-related properties of high performance concrete. Cement and concrete research, 42(1), 20-26.

[5] Kosmatka, S. H., Kerkhoff, B., & Panarese, W. C. (2002). Design and control of concrete mixtures (Vol. 5420, pp. 60077-1083). Skokie, IL: Portland Cement Association.

[6] Gowripalan, N. (1990). Effect of curing on durability. Concrete International, 12(2), 47-54.

[7] Ramezanianpour, A. A., & Malhotra, V. M. (1995). Effect of curing on the compressive strength, resistance to chloride-ion penetration and porosity of concretes incorporating slag, fly ash or silica fume. Cement and concrete composites, 17(2), 125-133.

[8] Montgomery, F. R., Basheer, P. A. M., & Long, A. E. (1992). Influence of curing conditions on the durability related properties of near surface concrete and cement mortars. Special Publication, 131, 127-138.

[9] Zain, M. F. M., & Matsufuji, Y. (1997). The influence of curing methods on the physical properties of high strength concrete exposed to medium temperature (20–50 ℃). In the Proceedings of the Fifth International Conference on Concrete Engineering and Technology, Kuala Lumpur, Malaysia.

[10] Zain, M. F. M., Safiuddin, M., & Yusof, K. M. (2000). Influence of Different Curing Conditions on Strength and Durability of High-Performance Concrete. ACI SPECIAL PUBLICATIONS, 193, 275-292.

[11] ACI COMMITTEE 305. 1-06, (2007). Specification for Hot Weather Concreting, American Concrete Institute Farmington Hills, MI.

[12] Christensen, B. J., Coverdale, T., Olson, R. A., Ford, S. J., Garboczi, E. J., Jennings, H. M., & Mason, T. O. (1994). Impedance spectroscopy of hydrating cement-based materials: measurement, Interpretation, and application. Journal of the American Ceramic Society, 77(11), 2789-2804.

[13] Gu, P., Xie, P., Beaudoin, J. J., & Brousseau, R. (1993). AC impedance spectroscopy (II): Microstructural characterization of hydrating cement-silica fume systems. Cement and Concrete Research, 23(1), 157-168.

[14] McCarter, W. J., & Afshar, A. B. (1988). Monitoring the early hydration mechanisms of hydraulic cement. Journal of materials science, 23(2), 488-496.

[15] Li, Z., Wei, X., & Li, W. (2003). Preliminary interpretation of Portland cement hydration process using resistivity measurements. Materials Journal, 100(3), 253-257.

[16] Xiao, L. (2007). Interpretation of hydration process of concrete based on electrical resistivity measurement, PhD Thesis, Hong Kong University of Science and Technology, Hong Kong.

[17] Ghoddousi, P., & Saadabadi, L. A. (2017). Study on hydration products by electrical resistivity for self-compacting concrete with silica fume and metakaolin. Construction and Building Materials, 154, 219-228.

[18] ASTM, C642. (2013). Standard test method for density, absorption, and voids in hardened concrete. ASTM International, West Conshohocken, PA.

[19] ASTM, C305 (2014). Standard practice for mechanical mixing of hydraulic cement pastes and mortars of plastic consistency. ASTM West Conshohocken, PA.

[20] Tazawa, E. I., Miyazawa, S., & Kasai, T. (1995). Chemical shrinkage and autogenous shrinkage of hydrating cement paste. Cement and concrete research, 25(2), 288-292.

[21] ASTM, C642. (2013). Standard test method for density, absorption, and voids in hardened concrete. ASTM International, West Conshohocken, PA.

[22] Flatt, R. J., Scherer, G. W., & Bullard, J. W. (2011). Why alite stops hydrating below 80% relative humidity. Cement and Concrete Research, 41(9), 987-992.

[23] Chen, L. & Ley, T.M. (2021). Real Time Measurement of Degree of Saturation and Tensile Strength of Mortar with Electrical Resistivity. Cement and Concrete Composites. (Submitted).

[24] Moradllo, M. K., & Ley, M. T. (2017). Quantitative measurement of the influence of degree of saturation on ion penetration in cement paste by using X-ray imaging. Construction and Building Materials, 141, 113-129.

[25] Moradllo, M. K., & Ley, M. T. (2017). Comparing ion diffusion in alternative cementitious materials in real time by using non-destructive X-ray imaging. Cement and Concrete Composites, 82, 67-79.

[26] Moradllo, M. K., Hu, Q., & Ley, M. T. (2017). Using X-ray imaging to investigate in-situ ion diffusion in cementitious materials. Construction and Building Materials, 136, 88-98.

[27] Moradllo, M. K., Sudbrink, B., Hu, Q., Aboustait, M., Tabb, B., Ley, M. T., & Davis, J. M. (2017). Using micro X-ray fluorescence to image chloride profiles in concrete. Cement and Concrete Research, 92, 128-141.

CHAPTER 4: Using Pulp Cure in the Field

4.1 Introduction

Pulp Cure is a novel way to apply wet curing to a bridge deck. The material can be applied in many different ways to the surface of a concrete bridge deck. Details about Pulp Cure application and test methods were presented in the final report for Part 1 of this project [1], this chapter provides an update on the application methods for Pulp Cure and reemphasizes some lessons learned in the field.

### 4.1.1 Previous Pulp Cure Mixtures in Oklahomas

The current Pulp Cure design uses a 30 lbs bale of recycled paper mulch or pulp with 60 lbs of water and 1.3 lbs of tackifier. This produces about 7.2 gallons of Pulp Cure or enough to cover 23 ft^2 with a ½" depth of coverage. This mixture used 4.2 lbs of pulp per gallon of water. Each gallon of Pulp Cure will cover about 3.2 ft^2 with ½" depth of coverage. It is recommended to use paper without dye so that it does not discolor the bridge. The paper with dye can be used but it will discolor the surface of the concrete.

The tackifier commonly used in Oklahoma is guar gum but other materials may be used. If a substitute material is used then the dosage rate of the tackifier needs to be adjusted. The test methods outlined in the final report from Part 1 [1] can be used to make this adjustment. Care needs to be taken while mixing the tackifier to make sure the material is well dispersed. If it is not, then the tackifier may clump and trap water. This makes the tackifier less effective. If the tackifier is premixed with the dry pulp then this will make mixing easier but it does not have to be this way. One challenge with premixed tackifier is that the material does lose its effectiveness over time and so the mulch must be used within a few months of receiving it.

The tackifier plays two important roles for the Pulp Cure. First, the tackifier keeps water from leaving the Pulp Cure mixture. The tackifier also helps hold the Pulp Cure together as a unit. This is especially important when applying the Pulp Cure on a slope. Figure 4-1 shows Pulp Cure on a slope with a sufficient dosage of tackifier and another Pulp Cure mixture with no tackifier.
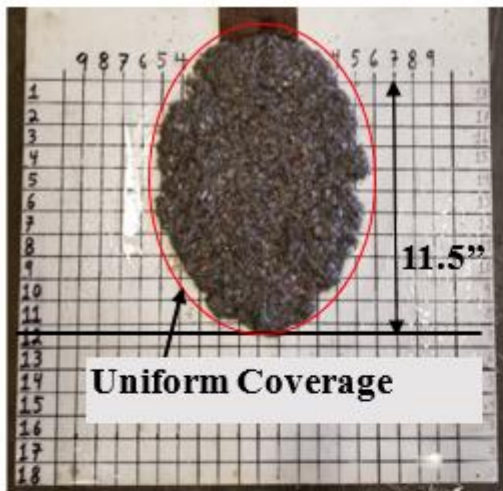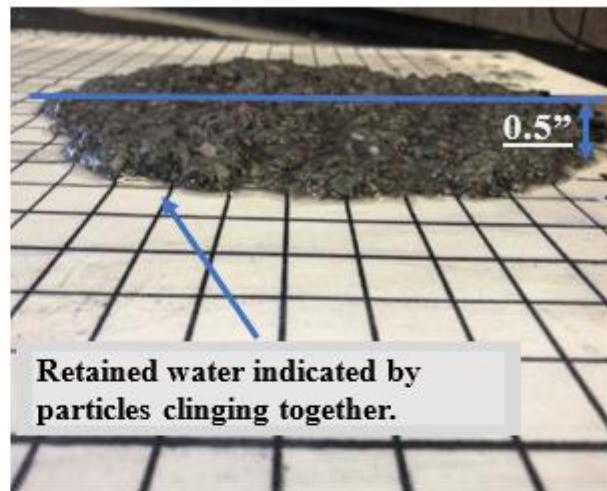
(a) 100% tackifier   (b) 100% tackifier
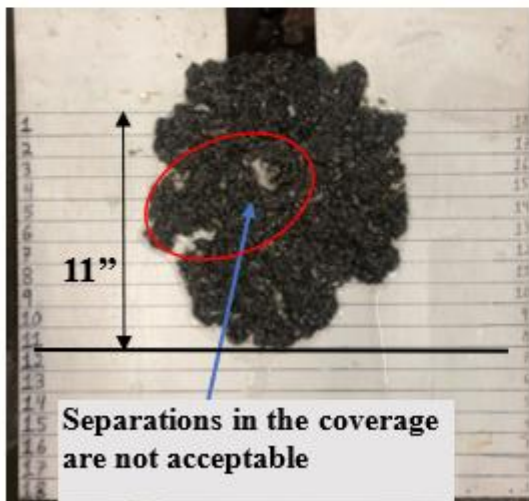
(c) 50% tackifier   (d) no tackifier

Figure 4-1 Performance on the slope test with three different dosages of tackifier.

The previous method of applying Pulp Cure used a five hundred gallon tank and mixed using two separate pumps designed to draw water from the base of the tank and discharge it back into the tank and therefore creating a recirculation or vortex process. This process was repeated until the mixture appears to be uniform and free of large, dry paper debris. Though this has proven to be an efficient process, the system can become overloaded with paper which requires manual breaking up of the bales. When this occurred it takes more time and effort, delaying the application to the concrete. Also, the tank is cumbersome to move from sight to sight.

Delivering Pulp Cure from the tank to the site has been completed by turning a valve that directs the return flow of one of the pumps to a tubing network. This network is connected to nozzles developed at Oklahoma State University specifically for this application. They are designed to have a spray width of 60° and to be mounted on a work bridge. The nozzle mounts are tilted upwards from the horizontal at approximately 30° which broadcasts the Pulp Cure over the concrete at a low angle of impact to preserve the surface as shown in Figure 4.2.

Several projects in Oklahoma were developed to use Pulp Cure and were written into specifications for projects. One of these projects occurred during the height of Covid 19 in Oklahoma and the plan sets were not followed and conventional curing was used on the bridge deck. Several other plan sets are in development or are issued while this report is being written.
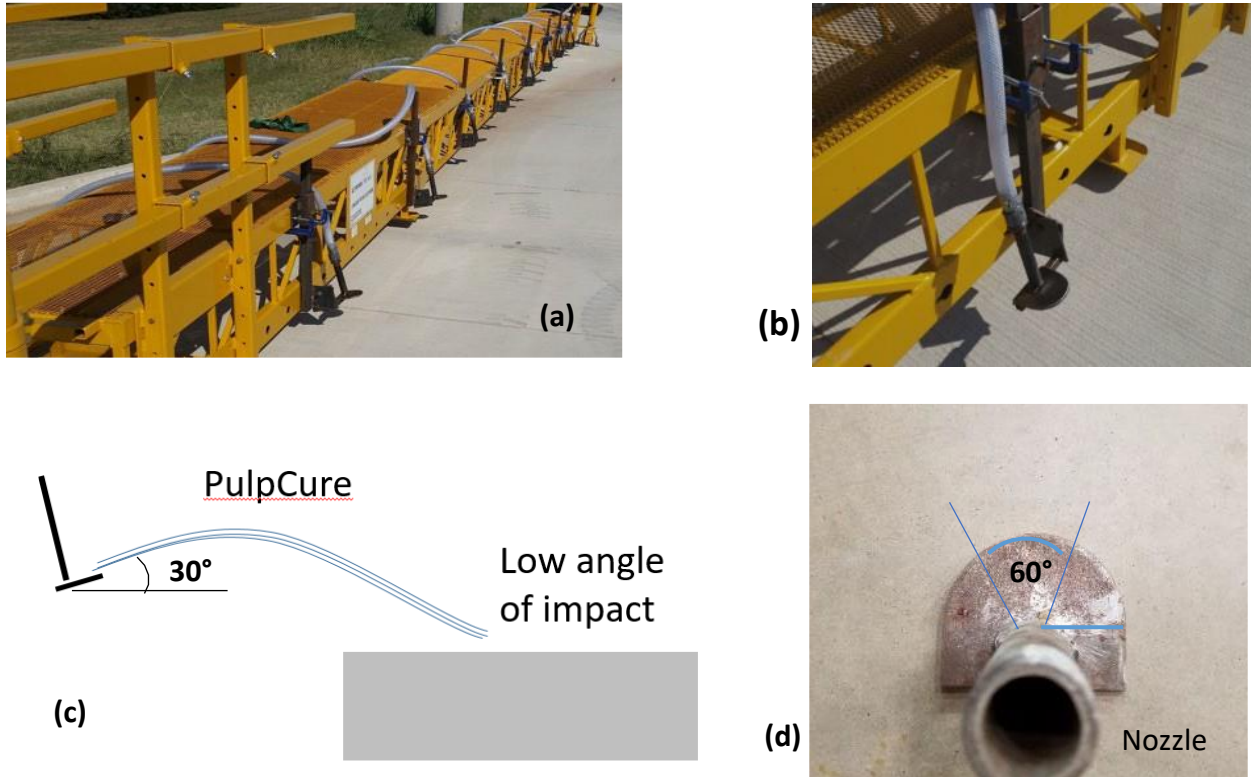
Figure 4-2 shows (a) entire work bridge with nozzles, (b) close-up of a nozzle, (c) diagram of pulp cure during placement, and (d) angle of nozzle.

4.2 Applications of Pulp Cure in Texas

By working with a contractor in Texas, a new mixing and placement method was developed for Pulp Cure. It should be noted that the application was to cure concrete that is made for slab on ground applications and roads. Because of this, it is easier for the contractor to maneuver next to the concrete with a trailer containing the equipment. The Pulp Cure was directly sprayed on the surface at about 5 h after initially placing the concrete. The slabs were also largely flat and they were covered quickly with plastic. Because of this the equipment and Pulp Cure mixture, and applicator looked very different than what was used in Oklahoma.

The contractor used two 285 gallon plastic containers. They filled each container with 250 gallons of water and added two 50 lb bales or 100 lbs of pulp per 250 gallons of water. This was 0.4 lbs of pulp per gallon of water. The bale was broken up by hand over for about two minutes and then mixed with a ½ horsepower drill for about 5 minutes. By using two tanks, one tank to be sprayed while another tank was mixed. This equipment is shown in Figure 4-3.

Figure 4-3 Mixing tank and ½ hp drill with a mixing vane.

This is 10% of the solids content per gallon of water. The Pulp Cure mixture has approximately 10% of the solids content per gallon of water than what was used in Oklahoma. This mixture used more water to make the material easier and faster to mix. It also minimized the mixing time and the chance for clogging in the lines. The downside with the method is that it would use more

water than what was used in Oklahoma to get the same solids content on the surface of the concrete.

The mixture in Texas also did not contain any tackifier because the slabs and roads were relatively flat. The material was sprayed directly onto the concrete with a 1/4" thickness at about 5h after concrete placement or when the concrete started to stiffen. The applied material is shown in Figure 4-4. The Pulp Cure was sprayed approximately 75' onto the surface of the concrete and it did not ruin the surface finish. A picture of the finished surface of the concrete is shown in Figure 4-5.

Figure 4-4 Pulp Cure applied at ¼" thickness and then covered in plastic.

Figure 4-5 The finished surface of the concrete after the Pulp Cure naturally was removed.

The Pulp Cure was applied at 50% of the thickness that was used in Oklahoma. This thin application was allowable because 6 mil plastic was used to immediately cover the surface of the concrete. A covered roadway is shown in Figure 4-6.

Figure 4-6 A concrete roadway that was cured with Pulp Cure and then covered with plastic.

The covered Pulp Cure stayed wet for more than 30 d with no additional water. The plastic was reused between uses. The pulp was not removed by the contractor. After removing the plastic, the Pulp Cure dried and then naturally was removed. Since the material was biodegradable then it did not hurt the environment.

The applicator used to apply the material was elegant. The contractor used a 7 hp pump with a 3" connection. A valve was added to the pump that could be switched quickly between the two mixing tanks. The pump outtake valve was reduced from 3" to 2" at the pump to go into a 2"

flexible hose for application. The 2" flexible hose was then reduced to ¾" at the end of the hose. This reduction to ¾" increased the pressure and allowed the Pulp Cure to be sprayed 75' in the air away from the nozzle. If there were any clogs during the application then this nozzle could be quickly cleaned by the operator. Overviews of the equipment are shown in Figures 4-7 and 4-8.

The contractor was very happy with this method to cure his concrete and has used it to cure more than 100,000 sf of concrete.
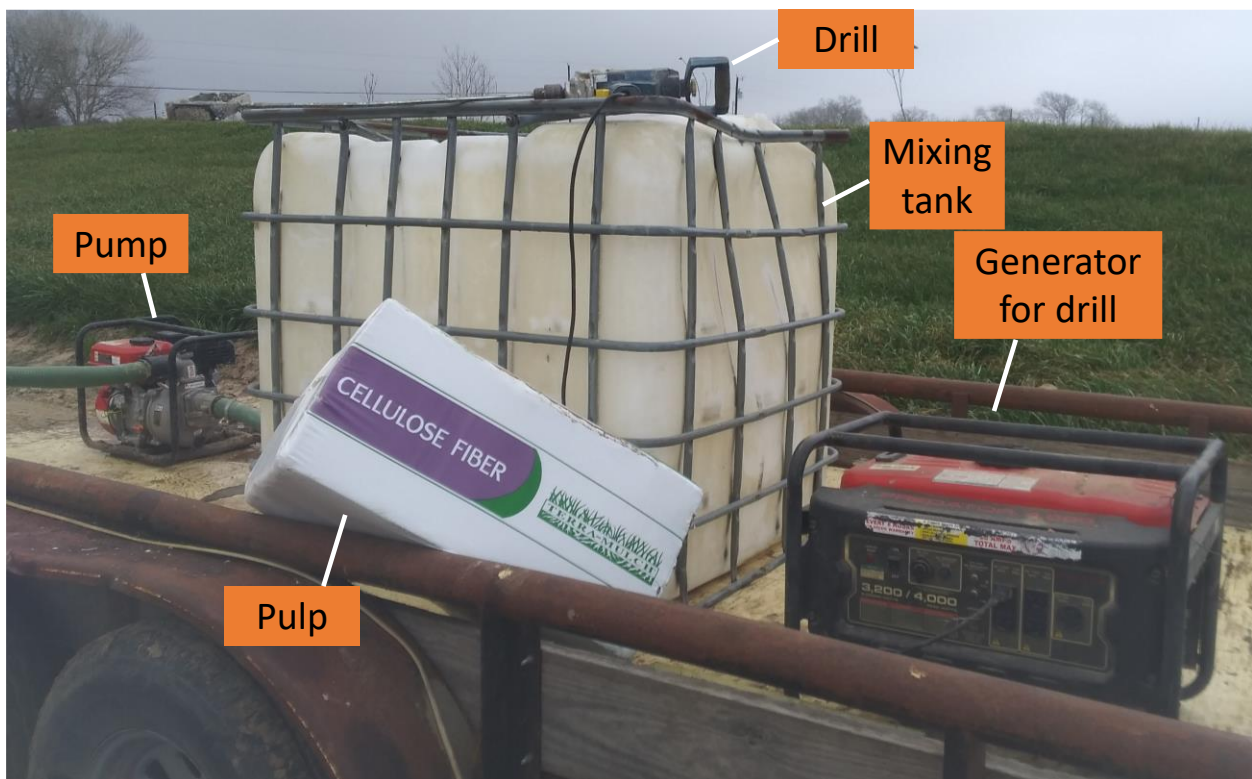
Figure 4-7 An overview of the equipment used to apply the Pulp Cure.
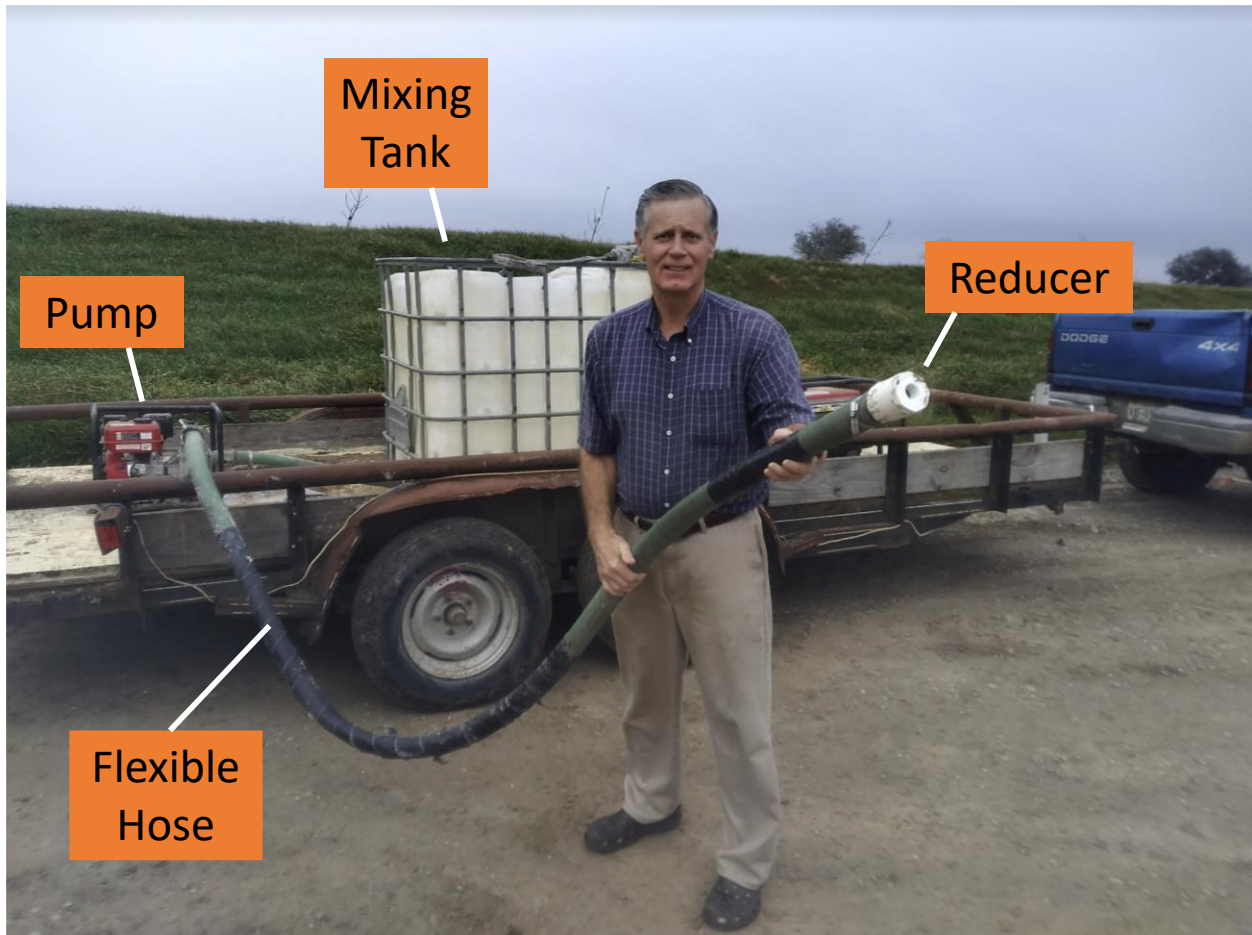
Figure 4-8 The applicator build and setup used to apply the Pulp Cure.

4.3 Lessons learned from Pulp Cure used in Texas

The Texas contractor was able to use simple equipment, a less expensive pulp, and a thinner application of pulp. The thinner application was possible because they quickly covered the surface of the concrete with plastic. They reported outstanding curing, easy application, and minimal impact on finishing. The contractor was very happy and would suggest that anyone use Pulp Cure to cure their concrete if they want an effective and easy way to cure concrete.

One challenge with adopting these methods in Oklahoma is that we have a specification that requires the placement of wet curing within 30 minutes of strike off. This requirement forced a lot of work to be done so that the Pulp Cure could be mixed and applied quickly. The research in the previous chapters of this report shows that the 30 minute curing requirement is more stringent than is necessary and the allowable curing window depends on the evaporation rate of the environment where the concrete is placed.

Also, in Oklahoma, the Pulp Cure was required to be applied in a ½" thick layer so that the contractor could wait until the next day to apply the plastic. If the contractor applies the plastic immediately then this layer could be reduced and this would save money, time, and labor to apply the Pulp Cure.

For the previous projects in Oklahoma, a special ordered pulp product was used with a higher processing level and no dye. The work in Texas shows that the paper for the Pulp Cure does not need to be anything special and any product can be used. Some material was used with an integral dye and it did discolor the surface of the concrete but it faded over time. This means a less expensive pulp could be used for applications in Oklahoma, but it is wise to avoid using an integral dye in the pulp. Some work may be needed to ensure the mixture could be placed on a slope. The tests outlined in Phase I of this project would be helpful to evaluate this.

Finally, the work in Texas shows that a very simple application method could be used to apply Pulp Cure. Sprayed application methods were not pursued in the past because the Pulp Cure had to be applied quickly after strike off and there was concern about damaging the surface of the concrete. Since the previous chapters have shown that it is possible to delay wet curing for many drying environments, a spray method may be a possible solution. If this is possible then it

greatly reduces the amount of specialized equipment that is needed to apply the Pulp Cure to the

surface of the concrete.

References

[1] Ley, MT., Wang, K., Li, JQ., Yang, G., Shao, Z., Hajibabaee, A., Khanzadeh, M., Behraven, A., Lloyd, Z., Cook, D. Effectiveness of Different Curing Methods For Bridge Decks. Final Report, FHWA-OK-15-05. Oklahoma Department of Transportation, 2018..

CHAPTER 5: Conclusion and Recommendation

5.0 Overview of Conclusions

This work introduces an electrical resistivity based method that can provide real time insight into the quality of curing in fresh concrete. This method has been used to compare the quality of different curing methods and also the timing required for different types of wet curing. The electrical resistivity measurements have been correlated with the porosity, DOS, strength of mortar samples, and the diffusion coefficient and shown good correlation for the materials investigated. An update of the improvement and usage of Pulp Cure in the field has been included. This method will reduce labor, save money, and make the method more practical. A summary of the primary conclusions of each chapter is contained below.

5.1 Using Electrical Resistivity to Predict early age DOS and tensile strength of mortar (Chapter 2)

A new technique of comparing curing effects using electrical resistivity at different depths was investigated in this study. The electrical resistivity was compared between wet curing, sealed curing, and air curing methods, at different depths within the sample and at different hydration times. These measurements are compared to the porosity, DOS, and tensile strength of the sample, and a linear relationship between resistivity and DOS is created for these materials. The following conclusions can be drawn for mortar between 12h and 72h:

- Resistivity corresponds to the degree of saturation, porosity, and tensile strength for a mortar mixture.

- A linear relationship is developed between resistivity and degree of saturation and this relationship changes as hydration proceeds.

- A bi-linear relationship exists between resistivity and porosity at a fixed DOS that is high enough to promote hydration.

- Wet curing samples showed uniform moisture gradients and had the highest degree of saturation and tensile strength of the samples measured. These samples also showed a 0.5% increase in the mass over the first 20 h of hydration.

- The air cured sample at 73°F and 50% relative humidity environment showed a significant drying gradient over the top 3.35 inch and the refinement of the pore structure stopped after 48 h. This sample also showed a 0.78% decrease in the mass over the first 70 h of hydration.

- The sealed sample showed a uniform moisture gradient and had a degree of saturation, porosity, and tensile strength that is between the wet cured and air cured samples. This sample showed only a slight change in mass during hydration that is likely from an imperfect seal.

- A porosity gradient was observed in all the mixtures regardless of the curing method used. This gradient is likely caused by differences in curing and also bleeding.

This work establishes a systematic method to use resistivity to rapidly and economically measure the in situ degree of saturation, porosity, and provide insights into the tensile strength of the concrete. This could provide a useful scientific and practical measurement technique for future work.

5.2 Early age hydration investigation on concrete with wet curing at different times (Chapter 3)

The influence of wet curing at different times was investigated in this study. The experiments were conducted under three different evaporation conditions for the first 72h of hydration. The diffusion

coefficient, porosity, DOS, and resistivity of the sample were measured and compared between curing methods. The following conclusions can be drawn:

- The electrical resistivity measurements are able to show the loss in moisture over time in all three drying environments. When wet curing was applied to the surface after 9h of drying for the samples in the 0.03 $lb/ft^2/h$ and 0.11 $lb/ft^2/h$ evaporation rate, the resistivity decreased to values similar to of the sample was never allowed to dry. However, in the 0.17 $lb/ft^2/h$ evaporation rate for at least 2h, the resistivity did not decrease to the same level as the sample continuously wet cured.

- At the 0.03 $lb/ft^2/h$ evaporation rate environment, delaying the wet curing for 6h did not impact the porosity of the sample. The diffusion coefficient was not impacted when the wet curing was delayed for 9h.

- At the 0.11 $lb/ft^2/h$ evaporation rate environment, delaying the wet curing for 3h did not impact the porosity of the sample. The diffusion coefficient was not impacted until the wet curing was delayed for 9h.

- The average porosity at 0.8 inch in depth is related to the resistivity gradient right before the application of curing in the 0.11 $lb/ft^2/h$ and 0.17 $lb/ft^2/h$ evaporation rate. The resistivity gradient was also useful in predicting the change in the diffusion coefficient in the 0.17 $lb/ft^2/h$ evaporation rate. This shows that the resistivity gradient in the sample during curing could be used to track changes in the surface porosity and the diffusion coefficient from drying.

This work would benefit from additional testing done in the field to verify the measurements and also to compare the predicted performance with a wider range of materials; however, the results show promise for establishing a method to measure the impacts of delaying wet curing in different environments on the porosity and diffusion coefficient of concrete.

5.3 Using Pulp Cure in the Field (Chapter 4)

The Texas contractor was able to use simple equipment, a less expensive pulp, and a thinner application of pulp. The thinner application was possible because they quickly covered the surface of the concrete with plastic. They reported outstanding curing, easy application, and minimal impact on finishing. The contractor was very happy and would suggest that anyone use Pulp Cure to cure their concrete if they want an effective and easy way to cure concrete.

One challenge with adopting these methods in Oklahoma is that we have a specification that requires the placement of wet curing within 30 minutes of strike off. This requirement forced a lot of work to be done so that the Pulp Cure could be mixed and applied quickly. The research in the previous chapters of this report shows that the 30 minute curing requirement is more stringent than is necessary and the allowable curing window depends on the evaporation rate of the environment where the concrete is placed.

Also, in Oklahoma, the Pulp Cure was required to be applied in a ½" thick layer so that the contractor could wait until the next day to apply the plastic. If the contractor applies the plastic immediately then this layer could be reduced and this would save money, time, and labor to apply the Pulp Cure.

For the previous projects in Oklahoma, a special ordered pulp product was used with a higher processing level and no dye. The work in Texas shows that the paper for the Pulp Cure does not need to be anything special and any product can be used. Some material was used with an

integral dye and it did discolor the surface of the concrete but it faded over time. This means a

less expensive pulp could be used for applications in Oklahoma, but it is wise to avoid using an

integral dye in the pulp.

Finally, the work in Texas shows that a very simple application method could be used to apply

Pulp Cure. Sprayed application methods were not pursued in the past because the Pulp Cure had

to be applied quickly after strike off and there was concern about damaging the surface of the

concrete. Since the previous chapters have shown that it is possible to delay wet curing for many

drying environments, a spray method may be a possible solution. If this is possible then it

greatly reduces the amount of specialized equipment that is needed to apply the Pulp Cure to the

surface of the concrete.

Appendix

Appendix A Seal the edge of mortar sample

The steps of sealing the mortar sample edge are shown in Figure 1 (a). Wrap the mold top with plastic. Two layers of plastic were used on each sample. (b) Tighten the plastic with rubber bands. Five rubber bands were used for each sample. (c) Fold the plastic into the mold along the mold edge. (d) Cover the plastic with fresh mortar from the same mixture. The coverage of mortar formed a concentric circle with an inner diameter of 4 in. and outer diameter of 6 in.
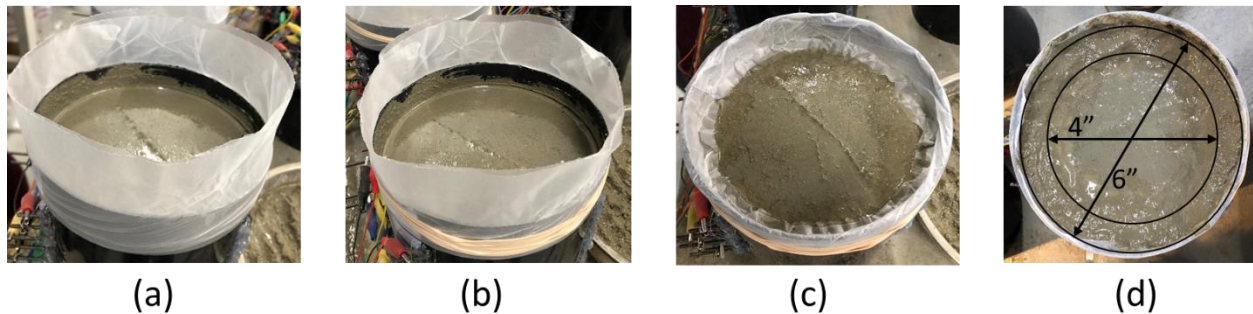

(a) (b) (c) (d)

Figure A- 1. Steps of sealing the sample edge: (a) wrap the mold top with plastic, (b) tighten the plastic with rubber bands, (c) fold the plastic along the mold edge, and (d) cover the plastic with mortar.

Appendix B Additional information of resistivity measurement

B.1 Supplementary hardware for the apparatus

Since the resistivity of the mortar samples at the early age of hydration was relatively low, it is necessary to adjust the AD5933 to the right range for the measurement. This is achieved by attenuating the excitation voltage from the AD5933 to reduce the signal current. As the result, an amplifier AD8531 was added into the circuit. An amplifier circuit can either amplify or attenuate the circuit signal. The purpose

of the amplifier circuit is to ensure the AD5933 system is within the linear range when measuring the small resistivity of the mortar sample. As a result, the external amplifier attenuates the peak-to-peak voltage at the output point of the AD5933 circuit, thereby reducing the signal current flowing through the sample and minimizing the effect of the output series resistance in the resistivity calculations [1,2].

An AD5933 chip contains one input and output channel, which is only able to measure the resistivity value of one pair of rods. Therefore, a dual 16-to-1 channel, serial controlled analog multiplexer ADG725 was used in the circuit to upgrade the measuring ability of the AD5933 from 1 dual-channel to 16 dual channels [3]. Five multiplexers were used in the circuit for this study. This allows 80 channels to be measured at once. As a result, 11 mortar samples with 7 layers in each sample were able to be measured at the same time. An SD card recorder was combined into the circuit to record the data.

B.2 Resistivity raw data process

The first step of calculating the resistivity value is to get the magnitude of the DFT on AD5933 at the known frequency point. The magnitude of the DFT is given by Equation 1B, where R and I are the real and imaginary impedance obtained from the real and the imaginary data register respectively on the AD5933. To convert the magnitude into an impedance, the magnitude needs to be multiplied by a scaling factor called the gain factor. The gain factor was obtained during the calibration of the apparatus with a known impedance connected with the circuit. In this study, a calibration resistor of 100 ohms and a frequency of 30 KHz was used and the gain factor was 8.54E-7 calculated from Equation 2B, where Magnitude $_{calibration}$ is the magnitude number obtained during calibration. With the gain factor, the unknown impedance at each depth of the mortar sample was calculated according to Equation 3B.

$$Magnitude = \sqrt{R^2 + I^2} \qquad\qquad Equation\ 1B.$$

$$Gain\ factor = (1\ /\ 100\ ohms)\ /\ Magnitude\ _{calibration} \qquad\qquad Equation\ 2B.$$

$$Impedance = 1 / (Gain\ factor \times Magnitude_{unknown}) \qquad\qquad Equation\ 3B.$$

Since the frequency range selected has forced the imaginary impedance to close to 0, the measured

impedance is also called the bulk resistance of the mortar sample.

Appendix C Coefficient of determination of the linear regression between resistivity and DOS

Table 1C. Parameters of the linear regression between resistivity and DOS in Figure 8

Hydration time	12h	24h	48h	72h
R^2	0.82	0.96	0.98	0.96
Slope(% / (Ω*inch))	-16031	-22334	-19452	-17277
Intercept(%)	105.29	120.71	127.60	128.89

Appendix D Load to strength calculation

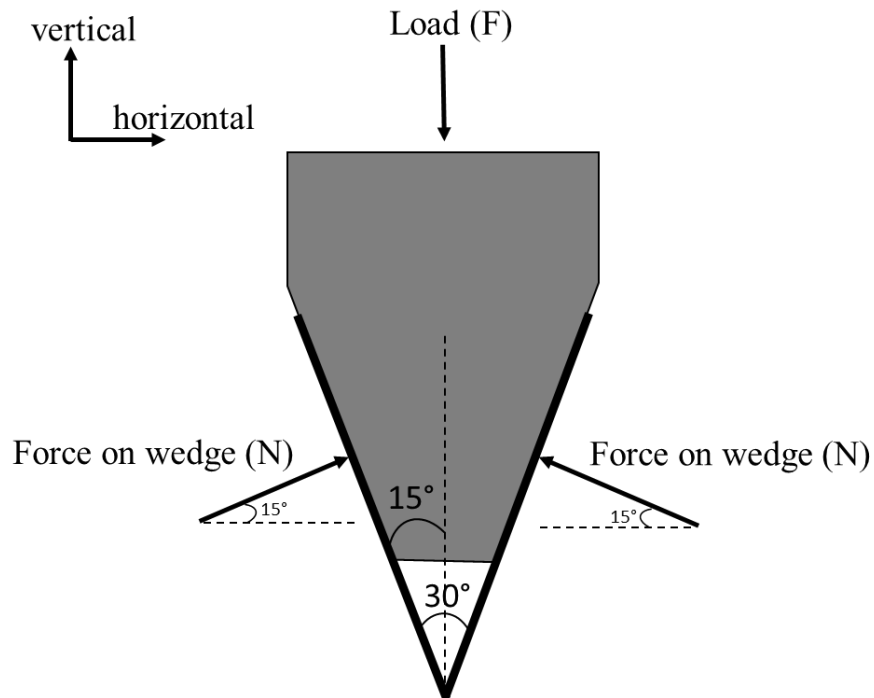The schematic of the free body diagram is shown in Figure 2D.

Figure 1D. Schematic of the free body diagram

Because there is no sliding observed during the test there is assumed to be no friction between the wedge

and the load platen. If the forces are summed in the vertical direction the force on the wedge (N) is equal

to 1.93F. This horizontal component of this force is 1.86F and since there is a wedge on the top and the

bottom of the beam the total horizontal force is 3.72F. The tension stress in the beam can be found by

dividing this load by the effective area at the point of the crack.

The diameter of the cylinder is 6 inch and the depth of each notch is 1 inch. This means the width of the

sample is 4 inch. Since each sample is 3 inch deep, the cross sectional area is 12 inch^2. An image of the
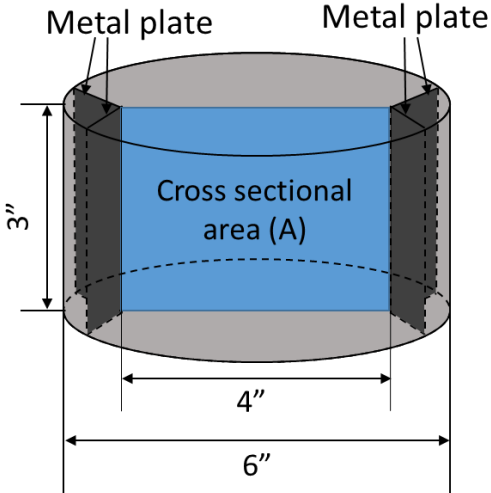
sample is shown in Figure 2D.

Figure 2D. Schematic of the cross sectional area of the mortar sample for splitting test

Appendix E Top porosity vs the resistivity gradient in the same graph.

The resistivity gradient versus porosity at 0.8 inches from the surface is plotted in Figure E-1. This shows the correlation of resistivity gradient and porosity for 0.03 lbs, 0.11 lbs and 0.17 lbs per square foot per hour.
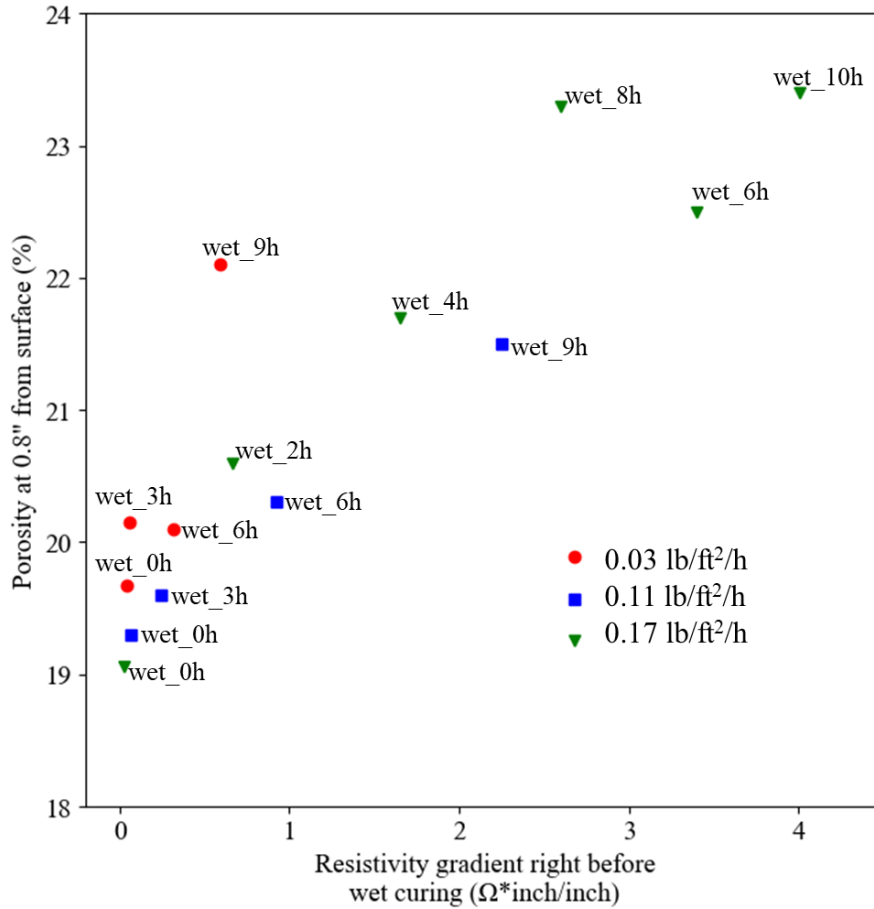

Figure E-1. Porosity at 0.8 inch from the surface versus the resistivity gradient right before wet curing is applied for different drying environments.

Reference

[1] Devices, A. (2007). AD5933 Datasheet. Available: http://www. analog. com/media/en/technical-documentation/data-sheets/AD5933. pdf.

[2] Device, A. (2008). AD8531 Datasheet. Available: https://www.analog.com/media/en/technical-documentation/data-sheets/AD8531_8532_8534.pdf

[3] Device, A. (2015). ADG725 Datasheet. Available: https://www.analog.com/media/en/technical-documentation/data-sheets/ADG725_731.pdf